5.6 Composite products generation

The last stage of the CRAMS chain (highlighted in **figure 5.24**) is dedicated to the generation of composite products from the radar network for weather monitoring. Part of the products, introduced in table 5.2 for the individual radars, are now applied to the mosaic, they are described in **table 5.4**.

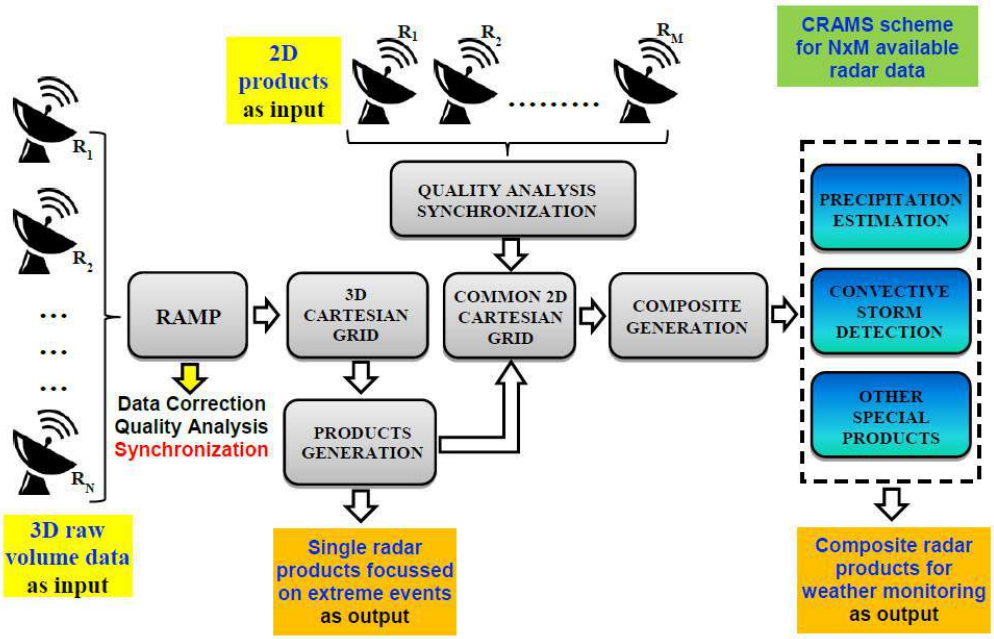

Figure 5.24 *Block diagram of the radar data processing and mosaicking algorithm (CRAMS), the modules described in this section are highlighted*

PRODUCT NUMBER	PRODUCT NAME	PRODUCT SYMBOL	SHORT DESCRIPTION
1	Vertical maximum of reflectivity	VMI	This product is useful for a quick surveillance of the composite area especially for convective precipitation to locate both mature and newly developing thunderstorm
2	Convective storm detection	CSD	The product is aimed at distinguish stratiform and convective areas in the composite being the latter linked to the most intense and dangerous phenomena
3	Surface Rainfall Intensity	SRI	This product estimates the ground instantaneous rainfall over composite coverage area in mm/h.
4	Surface Rainfall Total	SRT	This product estimates the cumulated rain over composite area in mm. It can issue warnings if the precipitation in a sub catchment region exceeds a threshold value.

Table 5.4 *Brief description of the composite products implemented within CRAMS chain*

Respect to the table 5.2, the composite products include the ones which can be obtained from reflectivity and precipitation 2D data only, being these products usually available as 2D input. Some examples of VIL and POH composite products will be shown in section 5.7 by using CRAMS-3D scheme. If we do not have 2D products as input we can generate VIL and POH at single radar level and then generate the composite. For this reason, the implementation of these products was

arranged in the CRAMS. The nowcasting (NOW) product has not been yet implemented in the composite but the module has been arranged in the CRAMS.
For each product described in the table 5.4 the description and the standard algorithms for their generation are described in detail in the **chapter 3 of deliverable 3.2.2**, so here they are not repeated.
In the figures below are shown some examples of application that refer to the mosaicking method of the highest total quality (method 6 of table 5.3). This technique, in fact, was found to have the best performance, as will be shown in the chapter 6.

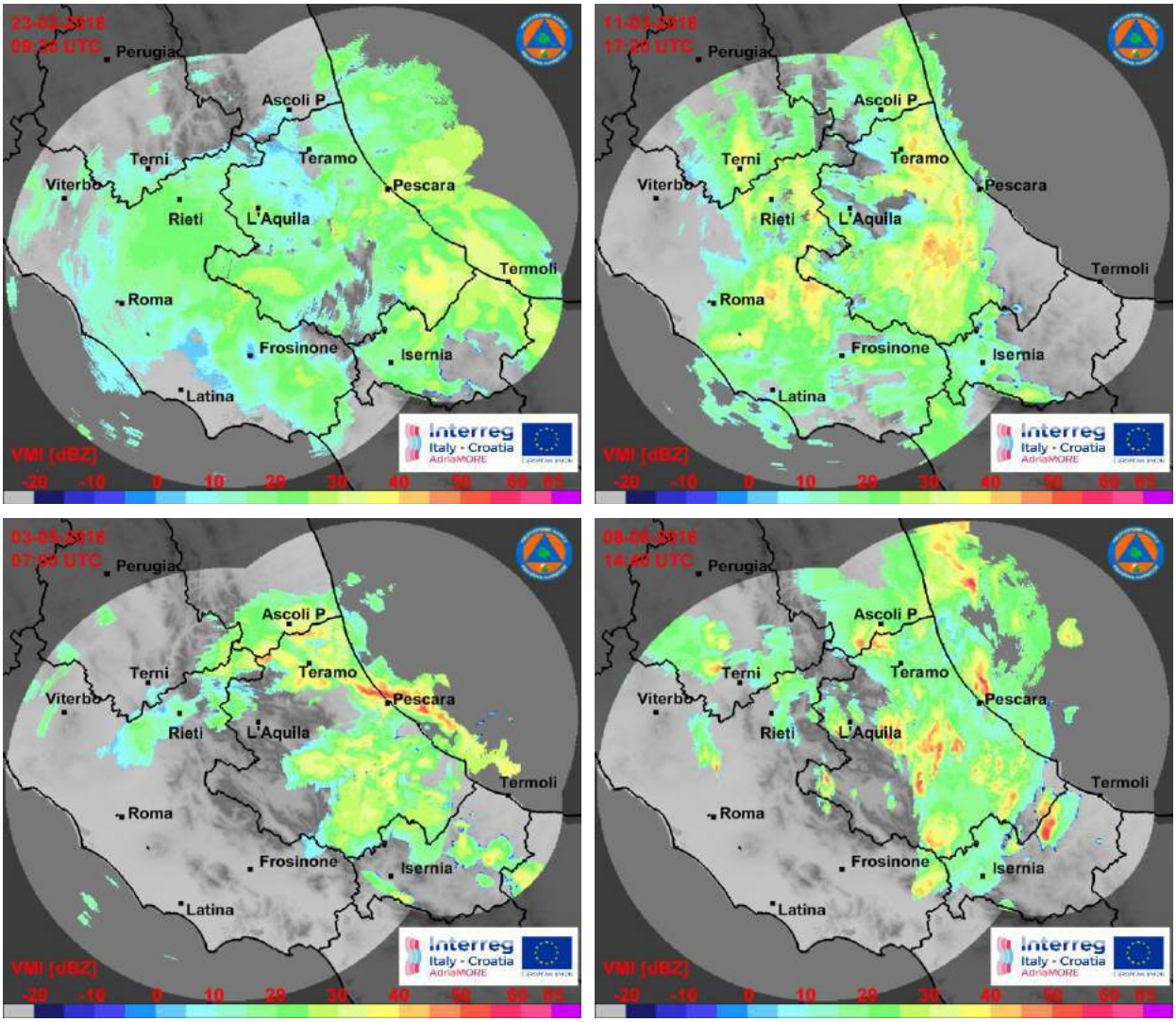

Figure 5.25 *Examples of* ***VMI composite product*** *for precipitation events occurred in the central Italy territory on February 23 at 9:30 UTC (top left), on March 11, 2018 at 17:20 UTC (top right), on May 3, 2018 at 07: 00 UTC (bottom left) and on June 8, 2018 at 14:40 UTC (bottom right)*

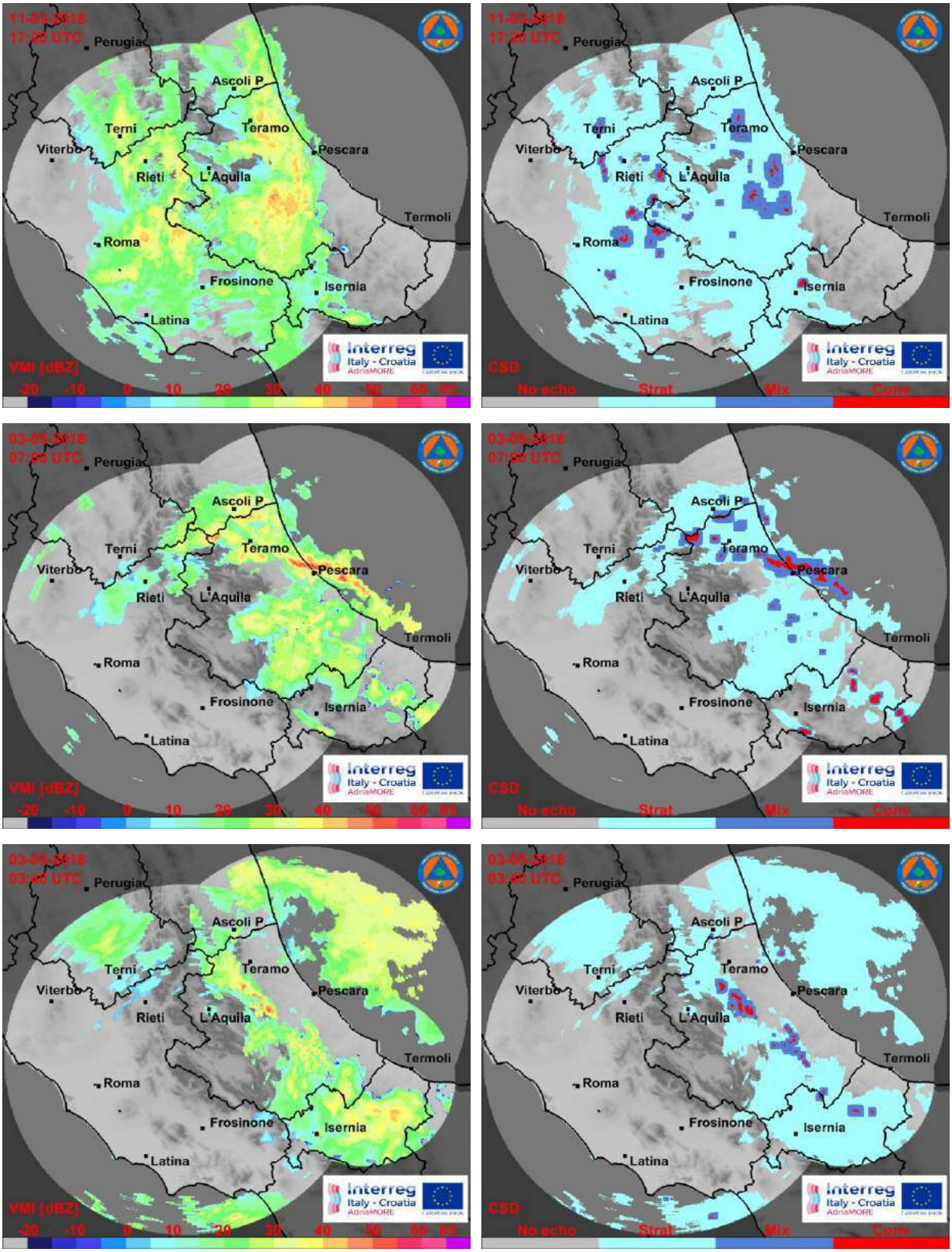

Figure 5.26 *Examples of* ***CSD composite product*** *for precipitation events occurred in the central Italy territory: in the left columns are shown the VMI while in the right columns the detection of convective centres: in the scale* ***Strat*** *stands for stratiform,* ***Conv*** *stands for convective and* ***Mix*** *stands for mixed precipitation*

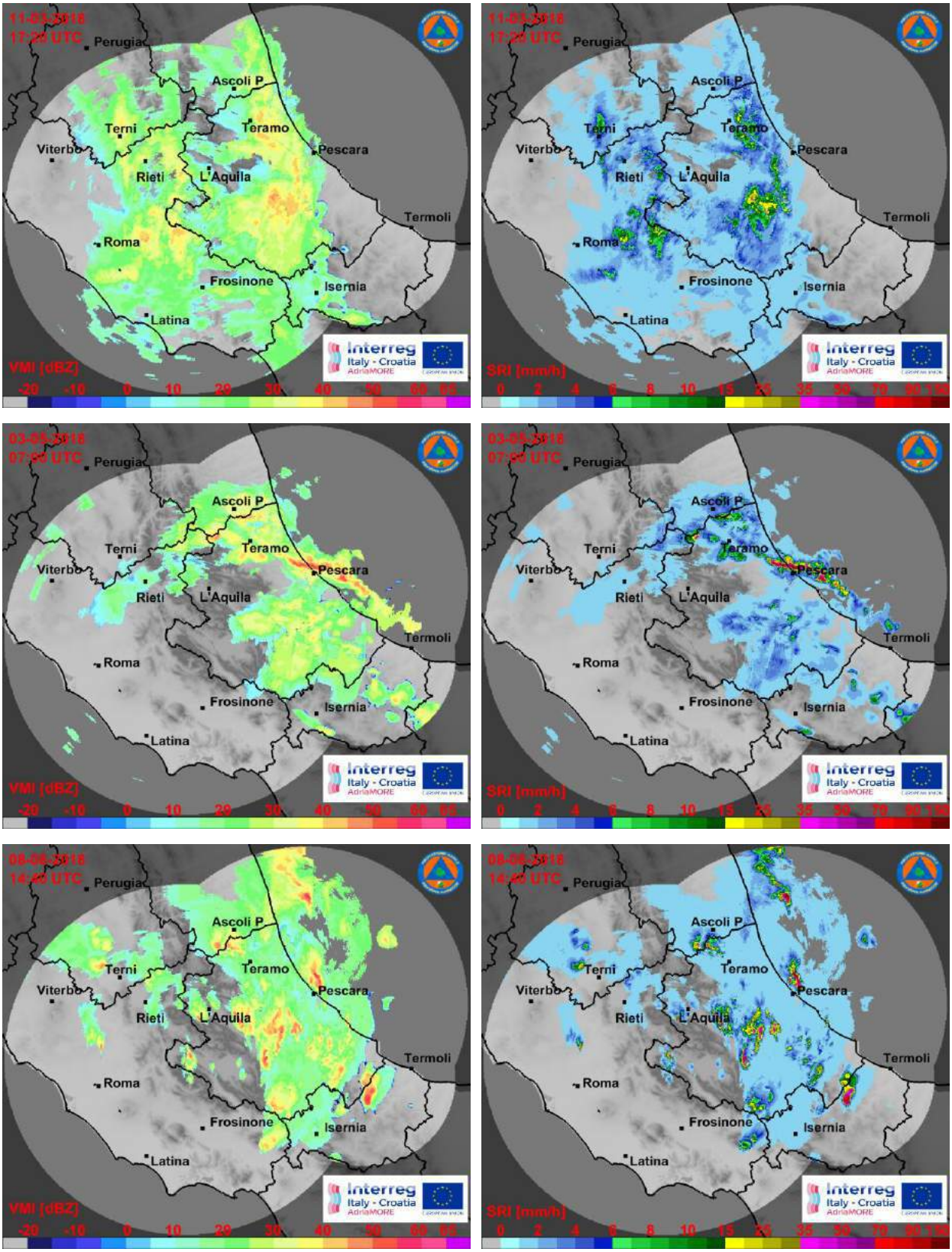

Figure 5.27 *Examples of* ***SRI composite product*** *for precipitation events occurred in the central Italy territory. In the left columns are shown the VMI while in the right columns the instantaneous rain estimation: look at the meaning of the threshold scale in table 5.5*

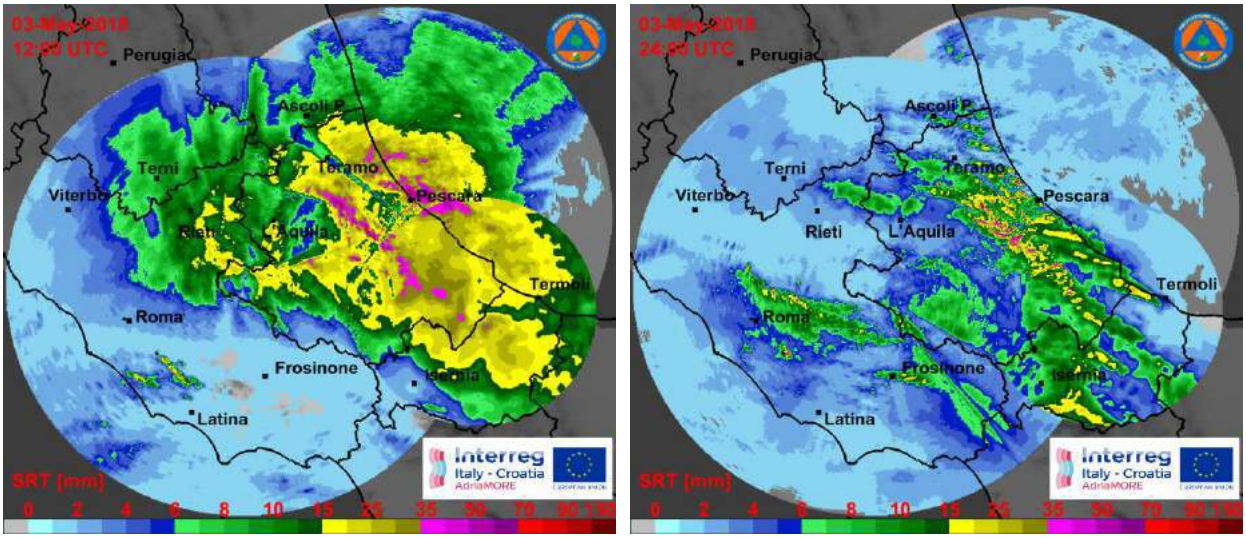

Figure 5.28 *Example of* ***SRT composite product at 12 hours*** *of accumulation in the central Italy territory: on May 3, 2018 from 00:00 to 12:00 UTC (left panel) and from 12:00 to 24:00 UTC (right panel)*

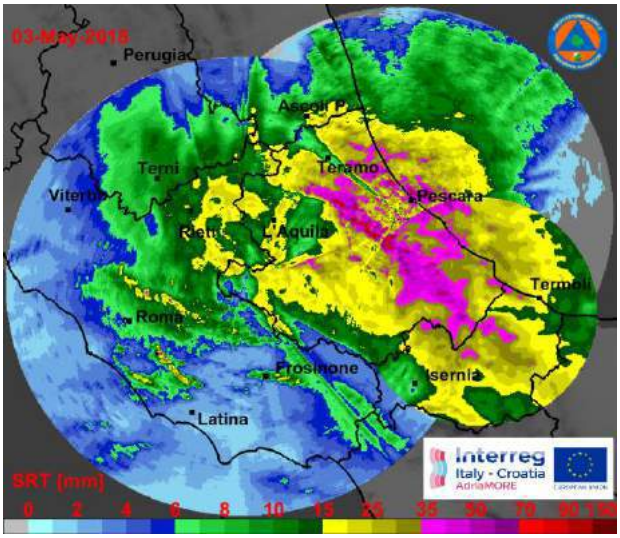

Figure 5.29 *Example of* ***SRT composite product at 24 hours*** *of accumulation in the central Italy territory on May 3, 2018 from 00:00 to 24:00 UTC*

Thresholds	Precipitation type	Colour
0-6 mm/h	weak	shades of blue
6-15 mm/h	moderate	shades of green
15-35 mm/h	strong	shades of yellow
35-70 mm/h	very strong	shades of purple
70-150 mm/h	violent	shades of red
> 150 mm/h	storm	shades of brown

Table 5.5 *Precipitation thresholds and related colours in the maps*

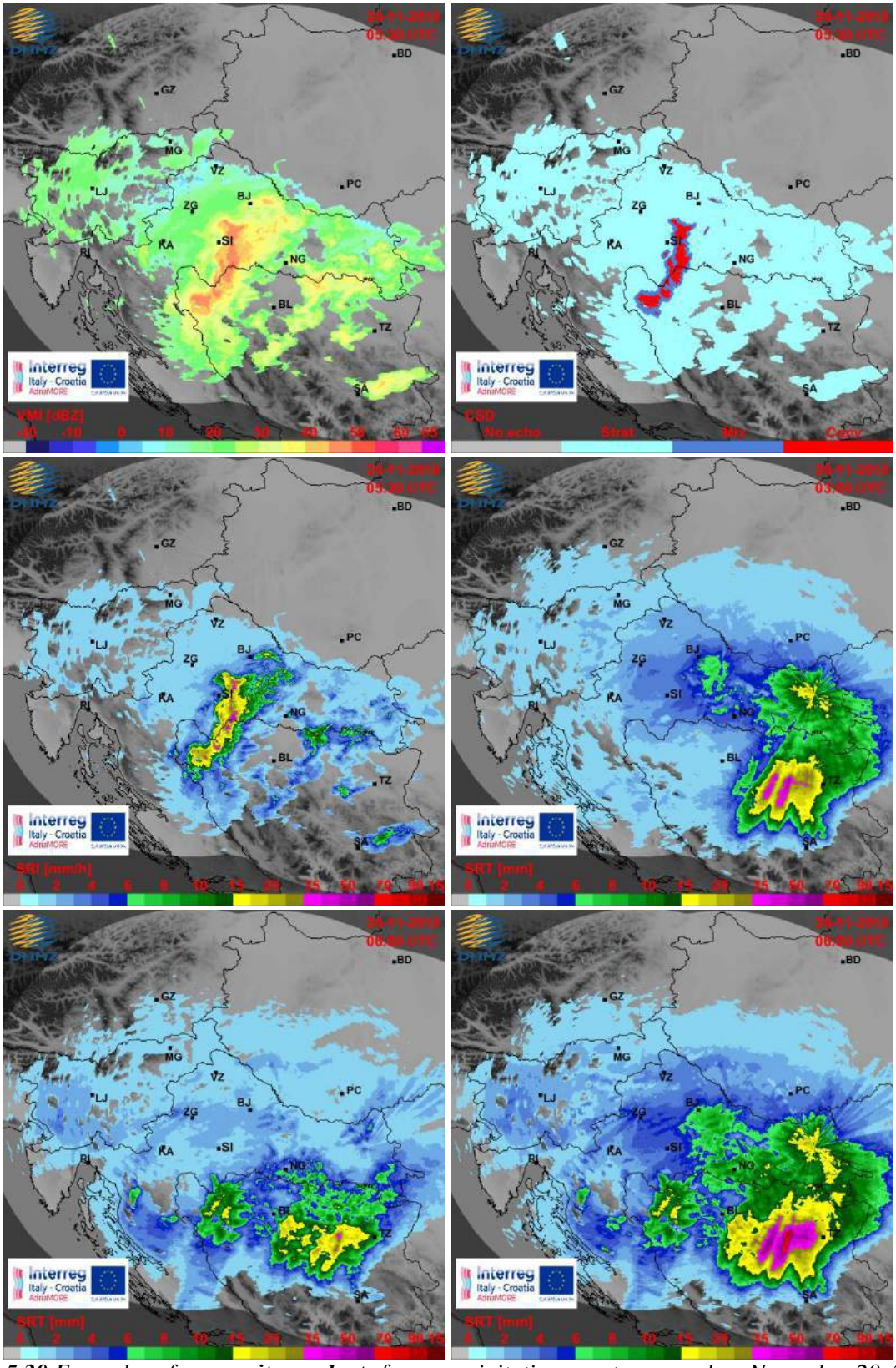

Figure 5.30 *Examples of* ***composite products*** *for a precipitation event occurred on November 20, 2018 in Croatian territory: VMI (top left), CSD (top left), SRI (centre left), SRT composite product at 3 hours of accumulation from 00:00 to 03:00 UTC (centre right) and from 03:00 UTC to 06:00 UTC (bottom left), SRT composite product at 6 hours of accumulation from 00:00 to 06:00 UTC (bottom right)*

5.7 Tridimensional mosaic scheme

As seen at the beginning of this chapter, starting from the measurements of several radars, the composite can be generated with:

a) **3D Mosaic**, that is directly from the volumes data acquired during the scanning of each radar (usually with 3D polar format);
b) **2D Mosaic**, that is starting from some specific products generated by each single radar such as VMI, SRI, SRT and other useful product.

The CRAMS scheme analysed up to now have been used for 2D mosaics technique to incorporate 2D products as input and for its better complexity and computational speed.
However, the advantages in the complexity and computational speed guaranteed by the 2D composite technique are at the expense of precision. This is because the composite products deriving from the 2D mosaic technique lack information on the height of the measurement which may be fundamental for meteorological observations of severe events and for the estimation of precipitation.
In order to maintain height information, a 3D version of the CRAMPS chain has been also designed, it can ingest three-dimensional data only (**figure 5.31**) in order to create a multi-radar mosaic directly in the 3D environment.
To maintain not only the height information but also the spatial resolution and the desired grid extension, it is preferable first create the specific 3D Cartesian grids comprising the data of each individual radar and then interpolate in a common 3D grid covering the entire mosaic domain, as illustrated in **figure 5.32 [Lakshmanan, 2014].**

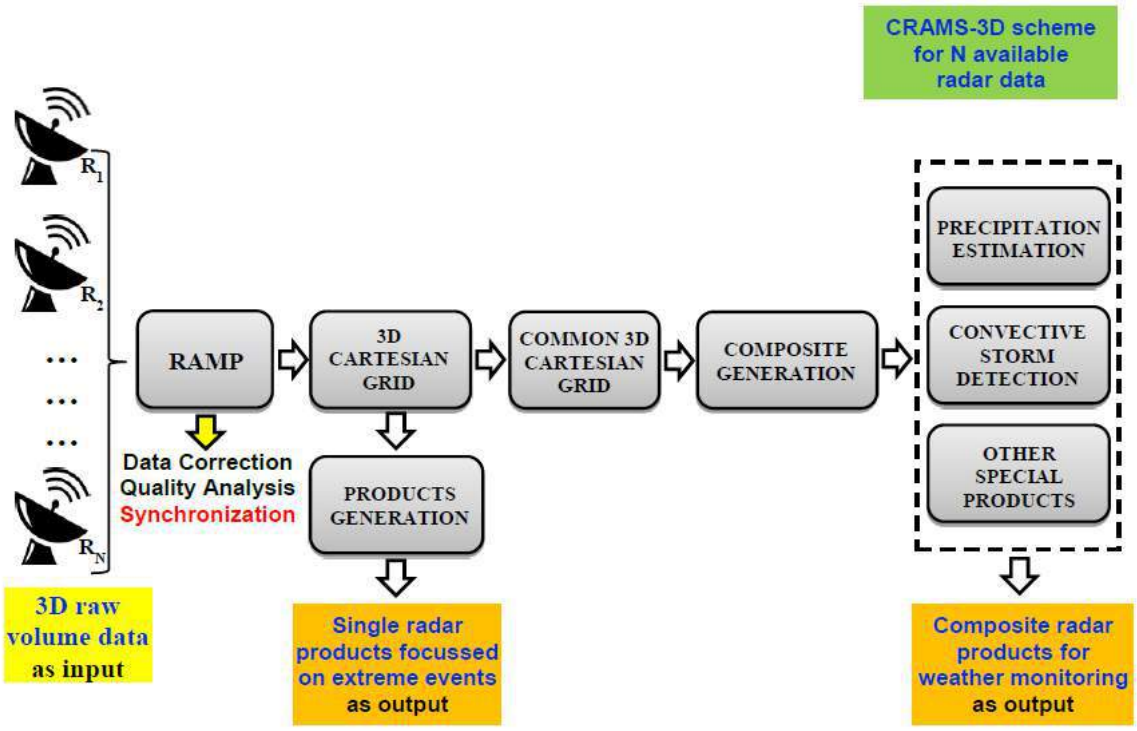

Figure 5.31 *Block diagram of the radar data processing and mosaicking algorithms using 3D mosaic technique (CRAMS-3D)*

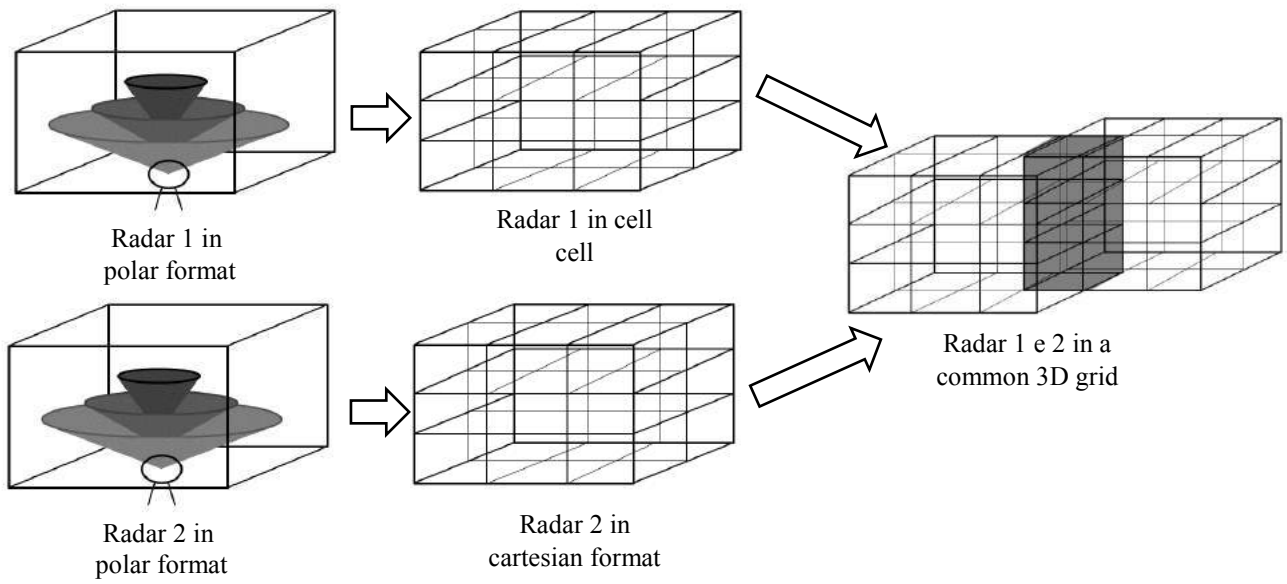

Figure 5.32 *The polar volumes of each single radar are combined on a specific 3D Cartesian grid and then mosaicked in a common 3D grid covering the entire mosaic domain*

Figure 5.33 shows the VMI products of the composite in the central Italy. The image on the left was obtained by combining the VMI of each single radar (2D Mosaic) while the image on the right the composite was generated directly in a three-dimensional environment (3D Mosaic) utilizing a same composition technique. What is noticeable is that the 3D composite image is more accurate even if the values are slightly scaled down. This is easily explained by the fact that in the 2D mosaic the composite is obtained from the VMI which by definition shows the maximum while in the 3D mosaic the composite is obtained directly from the volumetric reflectivity data.
In **figure 5.34** are shown the composite products, like VIL and POH, which requires the height information and thus the CRAMS-3D scheme for their generation.

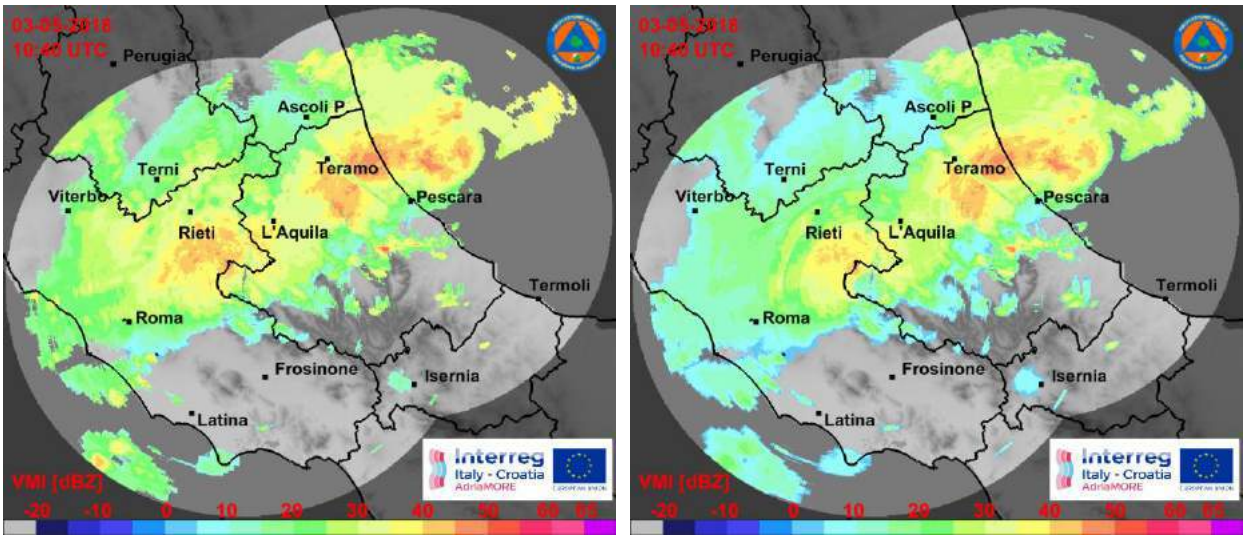

Figure 5.33 *Examples of VMI composite products made with 2D (left panel) and 3D (right panel) mosaic techniques for the event of May 3, 2018 at 10:40 UTC*

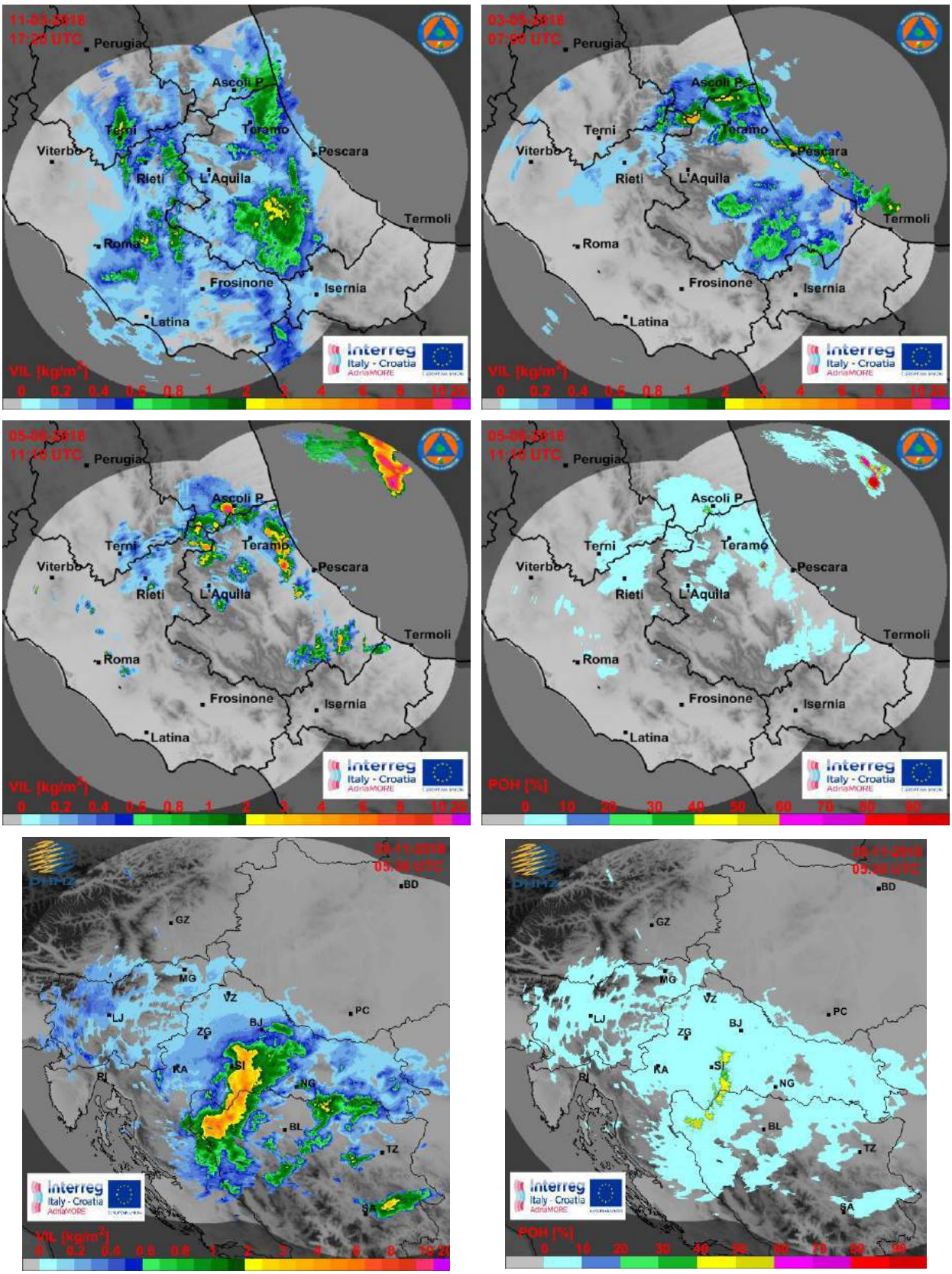

Figure 5.34 *Examples of* ***VIL and POH composite products*** *for precipitation events occurred in the central Italian (first two row) and Croatian territories (third row)*

6. PERFORMANCES ANALYSIS ON CASE STUDIES

Three case studies with different weather regimes have been selected to analysing the different merging strategies shown in the table 5.3. The first one is a stratiform event occurred on February 23, 2018. The second case, occurred on May 3, 2018, corresponds to a widespread event with moderate rainfall on the Adriatic coast. The third case, occurred on June 8, 2018, corresponds to a strong atmospheric instability that developed into several convective precipitation phenomena.

It is worth mentioning that stratiform precipitation falls from nimbostratus clouds (giving low radar reflectivity values in a large area), while convective precipitation falls from active cumulus and cumulonimbus clouds (giving high radar reflectivity values in circumscribed cells). These precipitation types may occur separately or entangled with each other in the same complex precipitation.

All case studies occurred in central Italy territory along Adriatic area and have been analysed by using the Abruzzo radar network thanks the large availability of the data.

6.1 Event occurred on February 23, 2018

The case study of February 23, 2018 is part of a perturbation originating in northern Europe. In fact, the synoptic situation of this day was characterized by a blocked anticyclone centred on the North Sea at 500 hPa and on the north of Scandinavia on the surface. Pressure minima were located on north-western Russia and west of the Mediterranean Sea. Such a configuration produced a wide flow of dry and cold continental air from Northeast Asia. On the other hand, a rather low surface pressure and a milder and humid air created unstable conditions over the Mediterranean region, as shown in **figure 6.1** by temperature and pressure map at 00:00 UTC on February 23.

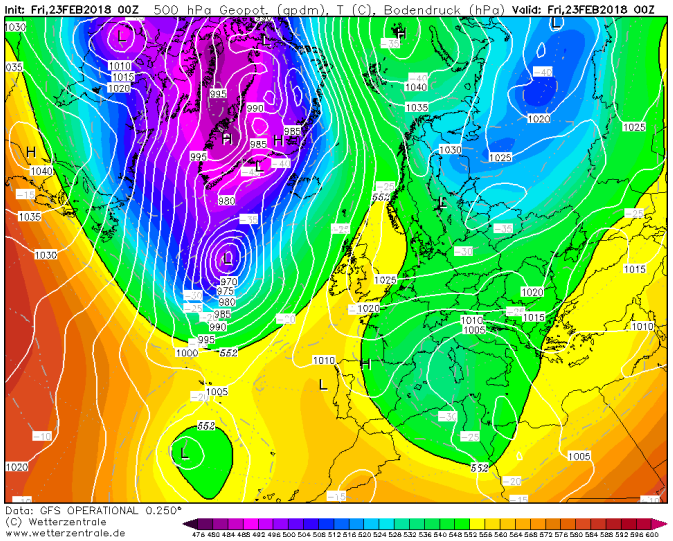

Figure 6.1 *GFS map of geopotential in gpdm at 500 hPa (shaded colour), temperature in ° C (dashed-point isolines in gray) and ground pressure in hPa (white isolines) at 00:00 UTC on February 23, 2018*

The trend of the event was also highlighted by the Italian rain gauge network. The precipitation accumulated during the 24 hours (**figure 6.2**) shows moderate rainfall with located areas with peaks of about 40mm/24h, indicated by black arrows, in the mountainous areas of the Apennines, on the border with Marche and Molise region, and along the Tyrrhenian coast of Lazio region.

The data of the Italian rain gauge network are collected by the Italian Department of Civil Protection (DPC) and distributes through DEWETRA web-based software.

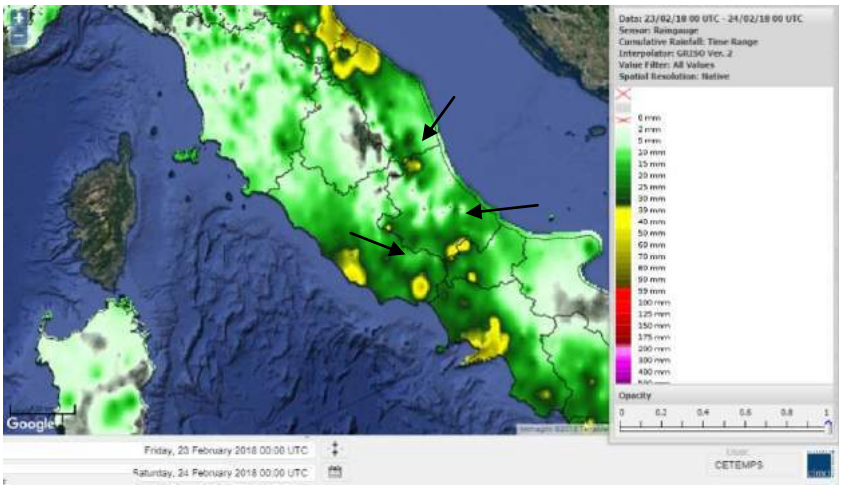

Figure 6.2 *Map of ground precipitation accumulated in 24 hours starting from 00:00 UTC on February, 23 2018 from the DEWETRA DPC Italian rain gauge network*

Due to low rain-rate values, relevant attenuation phenomenons are not present in the X-band radar measurements. In the overlapped observation areas both X-band and C-band radar have a good characterization of the precipitation cells, making it rather difficult to compare the mosaic methods by visual comparison.

In the following figures the mosaic methods are numbered following the same scheme of table 5.3.

All the weight functions used are monotonically attenuated by moving away from the radar (**figure 6.3**), differentiating themselves by the speed with which they decrease. In decreasing order, we have: the quadratic weight (method 10 of table 5.3), the linear weight (method 3 of table 5.3), the exponential weight (method 4 of table 5.3) and that linked to the inverse power of distance (method 5 of the table 5.3). The weights that decrease faster can cause underestimation in the farthest overlapping points of the mosaic.

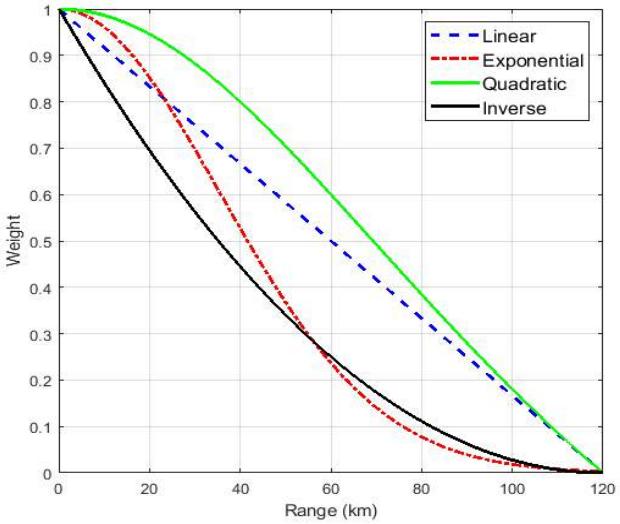

Figure 6.3 *Trend according to the range of the weight functions used in the mosaic process*

In the composite of the radar images, considering the maximum value of the measurement is a conventional choice (**figure 6.4a**, panel 2) but also the Mean algorithm (**figure 6.4a**, panel 1), with the advantage of compensating for data discrepancies, has good behaviour.

The minimum PIA method gives variable results especially with radar systems with different wavelengths that provide a different attenuation correction. **Figure 6.4b**, panel 7, for example,

shows lower reflectivity values in the overlap area, due to the dominant contribution of radars with low PIA values, as can happen in cases of widespread precipitation and with a short path from the point of measurement.

The method based on the principle of the quality (**figure 6.4b**, panels 6, 8 and 11) is a good compromise between the tested methods as it is inclusive of the main problems affecting the data of the various radars.

The composites obtained by weight functions (depending on the distance of the various radars at the point of the grid in common) are rather similar: the distance from the radar is used as a quality indicator.

Finally, the Weighted Quality and distance algorithm (**figure 6.4b**, panel 11) employs the Quality value, propagated from the radar, to compensate the underestimation of distance weight far from the radar site. For this event, it does not present particular discrepancies in the overlapping areas, guaranteeing the visualization of the most intense precipitation cells.

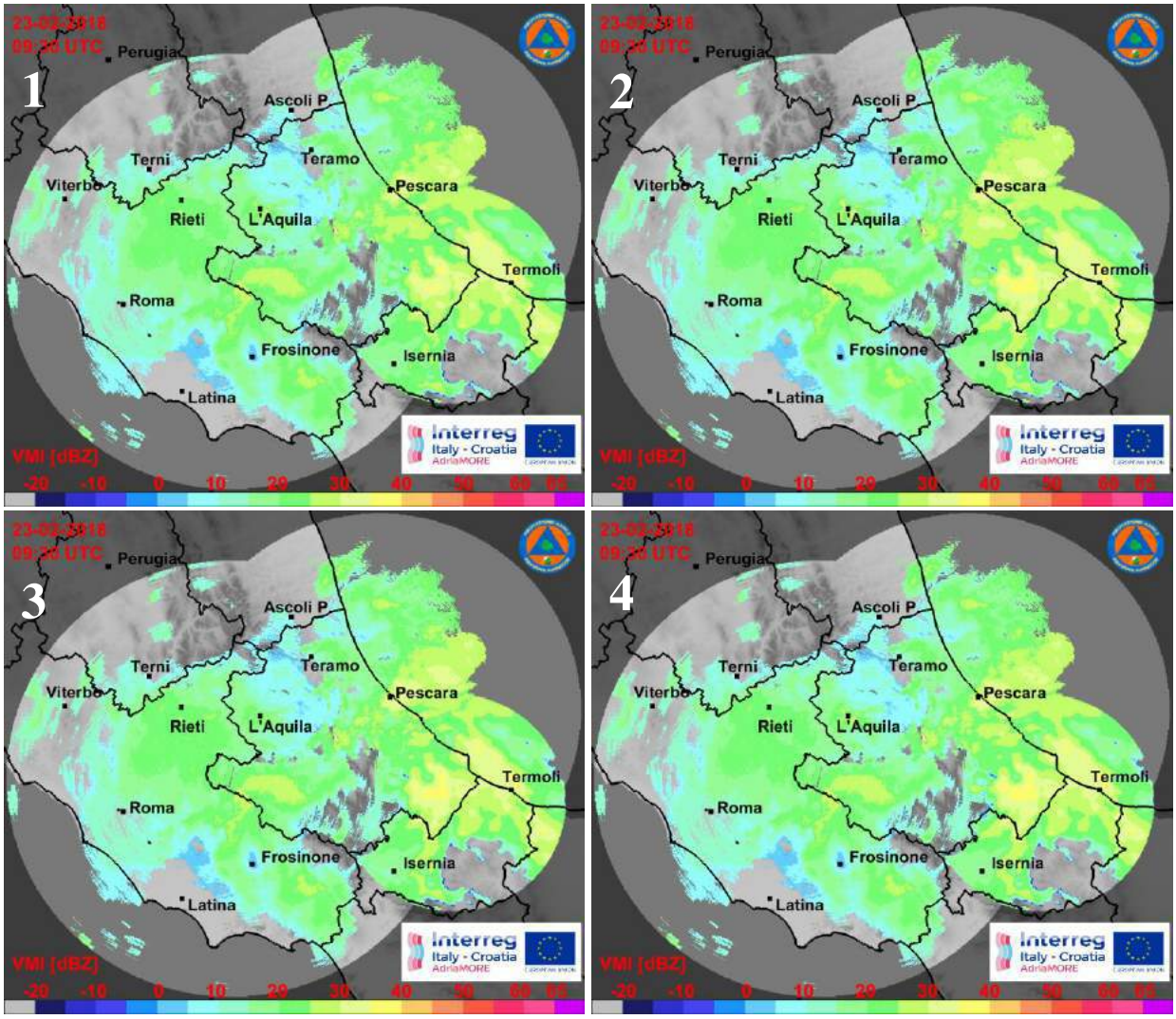

Figure 6.4a *Example of reflectivity composite techniques in the composite domain on February 23, 2018 at 09:30 UTC. MEAN reflectivity (1), MAXIMUM reflectivity (2), LINEAR WEIGHTED with the distance (3) and EXPONENTIAL WEIGHTED with the distance (4)*

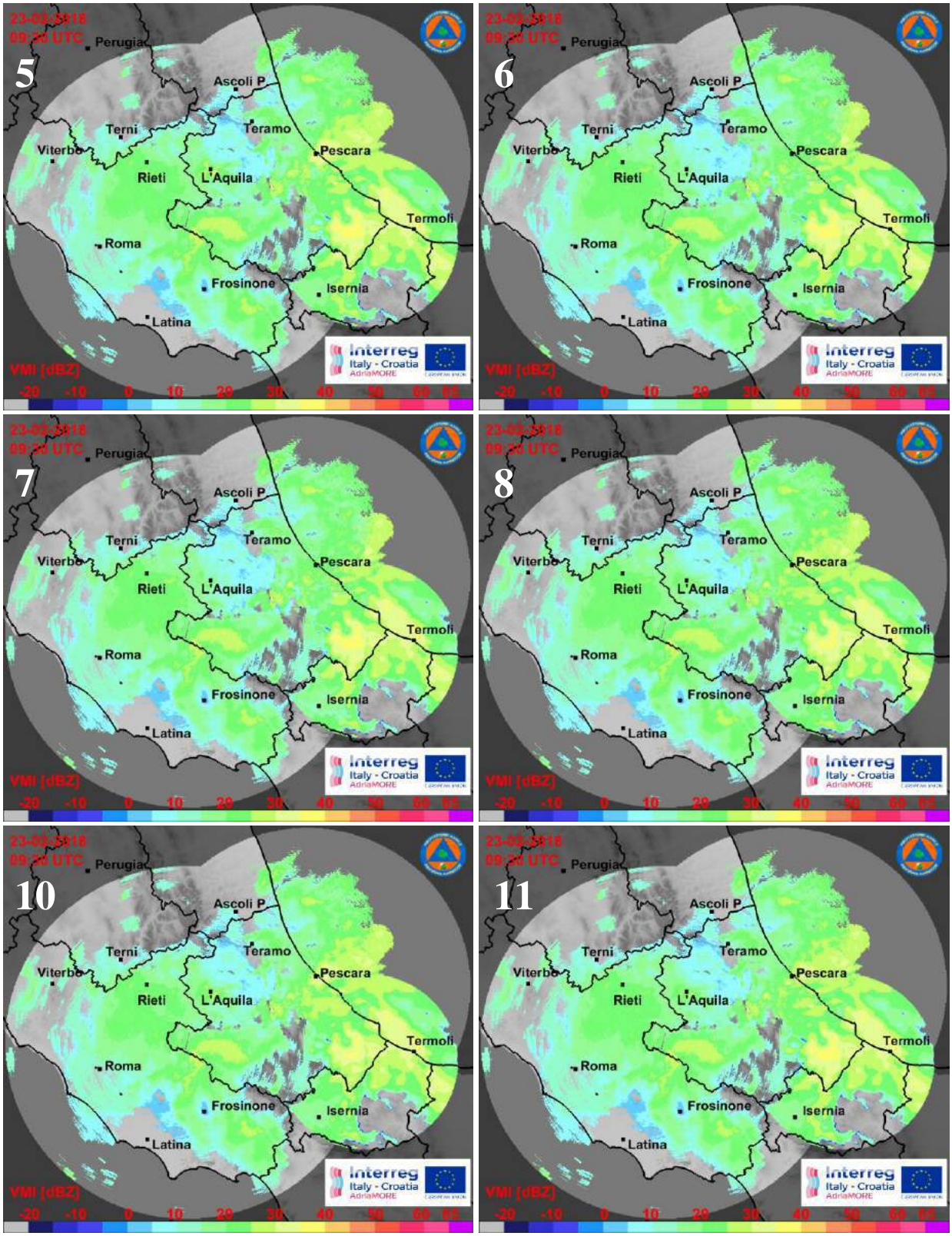

Figure 6.4b *Example of reflectivity composite techniques in the composite domain on February 23, 2018 at 09:30 UTC. INVERSE DISTANCE WEIGHTED (5), MAXIMUM QUALITY (6), MINIMUM PIA (7), QUALITY WEIGHTED (8), QUADRATIC WEIGHTED with the distance (10) and QUALITY-DISTANCE WEIGHTED (11)*

In the **figure 6.5** are shown some examples of the composite radar products (SRI, CSD, VIL and POH) obtained with the Maximum Quality algorithm (method 6 of table 5.3).
The maps are in-line with the stratiform characteristic of the precipitation that is low values of SRI and VIL as well as absences of convective areas in the CSD and null POH values.

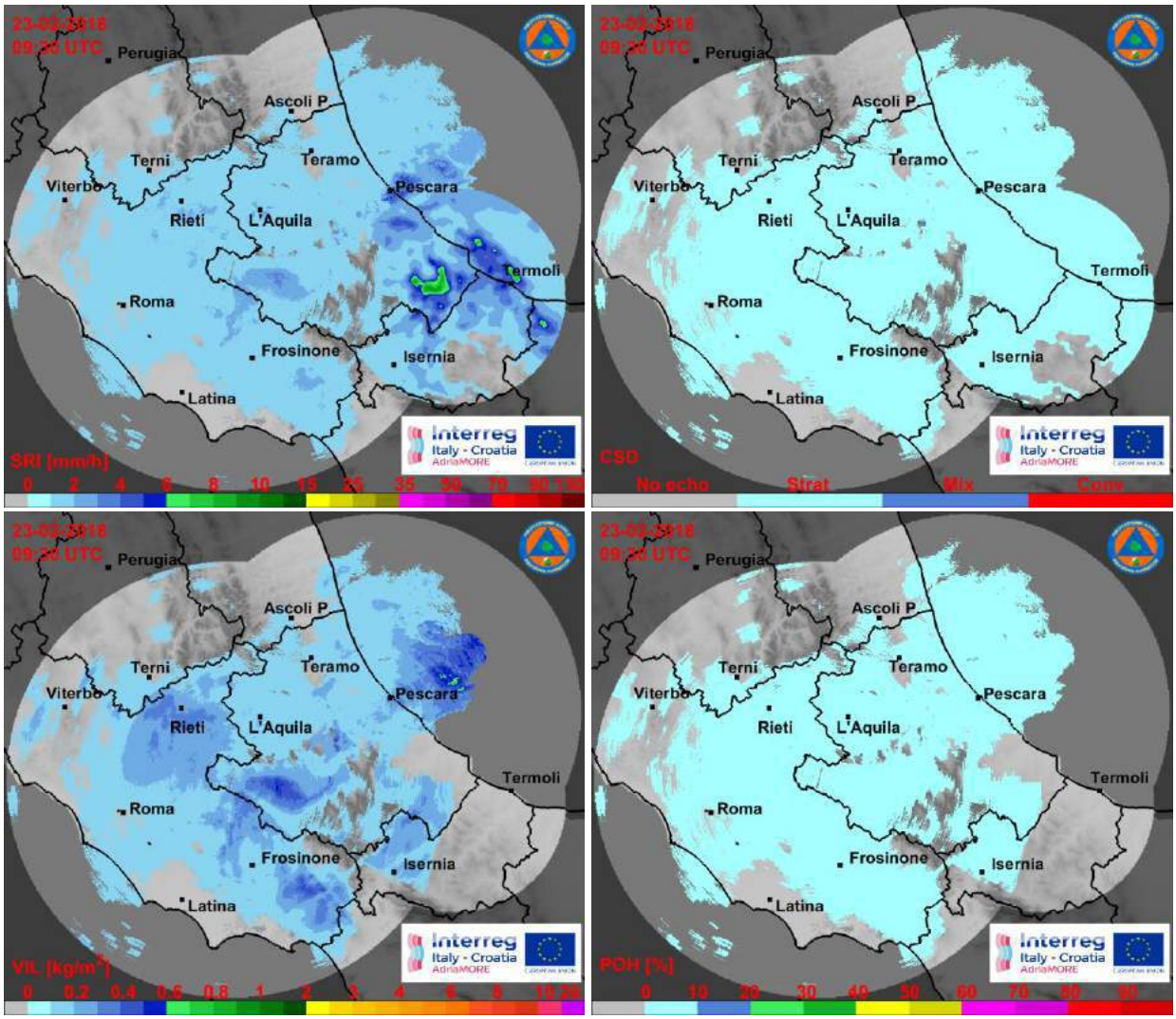

Figure 6.5 *Examples of composite radar products on February 23, 2018 at 09:30 UTC: SRI (top left), CSD (top right), VIL (bottom left) and POH (bottom right)*

6.2 Event occurred on May 3, 2018

The case study of May 3, 2018 was characterized by a low pressure at high altitude (a so-called *cut-off low*) located over the central area of the Tyrrhenian sea, as shown in **figure 6.6**, which resulted in heavy rainfall and strong winds coming from the eastern quadrants.

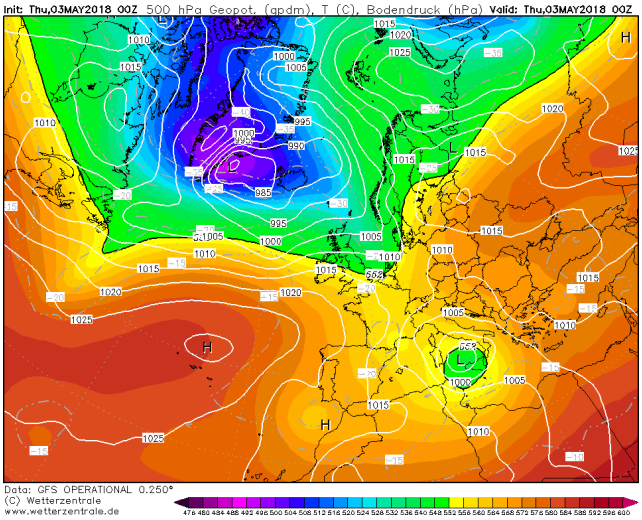

Figure 6.6 *GFS map of geopotential in gpdm at 500 hPa (shaded colors), temperature in ° C (dashed-point isolines in gray) and ground pressure in hPa (white isolines) at 00:00 UTC on May 3, 2018*

The event highlighted local rain showers and storm phenomena, especially along the eastern slopes of the mountains. As can be appreciated from **figure 6.7**, there were two significant cells of 100 mm/24h (indicated by the arrows in black) in correspondence with the major peaks of Gran Sasso mountains, while on the entire eastern part of the region the rain gauges recorded rainfall between 40 and 60 mm/24h (pattern in yellow).

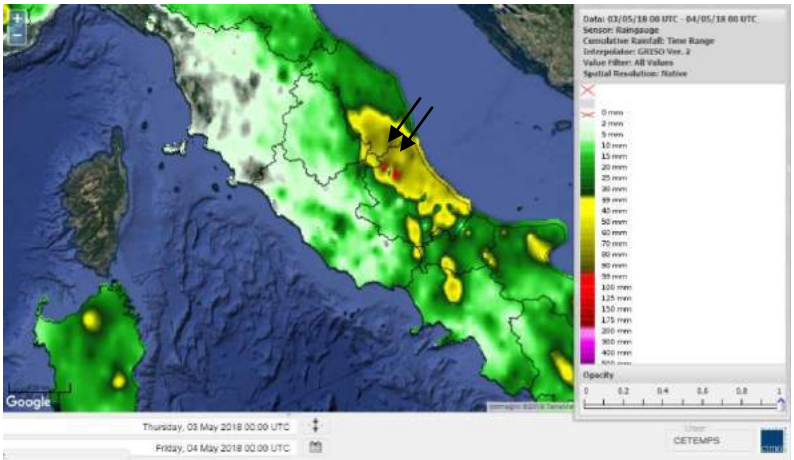

Figure 6.7 *Map of ground precipitation accumulated in 24 hours starting from 00:00 UTC on May 3, 2018 from the DEWETRA DPC rain gauges network*

In the **figure 6.8** are shown some examples of the composite radar products (SRI, CSD, VIL and POH) obtained with the Maximum Quality algorithm (method 6 of table 5.3). The maps are in-line with the mixed characteristic of the precipitation that is medium values of SRI and VIL as well as the presence of few convective areas in the CSD and low POH values.

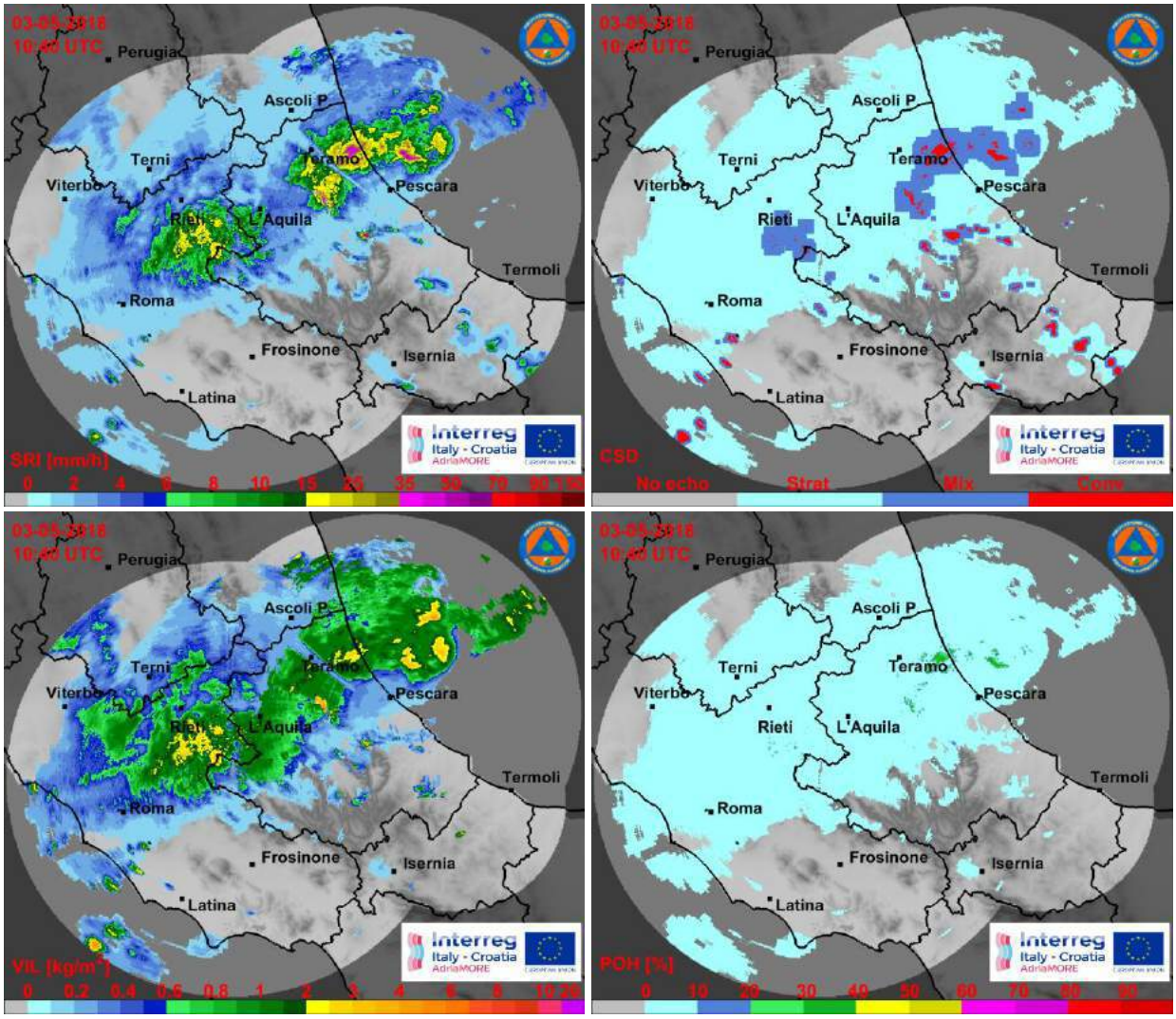

Figure 6.8 *Examples of composite radar products on May 3, 2018 at 10:40 UTC: SRI (top left), CSD (top right), VIL (bottom left) and POH (bottom right)*

Local rain showers and storm phenomena have been well identified only by the Maximum algorithm (method 2 of table 5.3) and by the Maximum Quality algorithm (method 6 of table 5.3), shown respectively in **figure 6.9a** panel 2 and **figure 6.9b** panel 6, while the other cases show lower reflectivity. The Maximum method, retaining the highest reflectivity intensities in the data fields, possibly mitigates attenuation losses due to regions of intense rainfall but could provide a biased estimate due to radars that provide higher reflectivity values as a result of calibration differences.
The applied methods do not impose any smoothing when creating a mosaic from multiple radars. However, discontinuities may appear at the boundaries of the radar range. **Figure 6.9b**, panel 7, shows the lower reflectivity values in the overlapping area presumably due to low PIA values as expected in a widespread case.
The data of the entire day of May 3 will then be used to evaluate the methodology of mosaicking by comparing the precipitation estimates with the measurements of rain gauges and described in detail in the chapter 6.4.

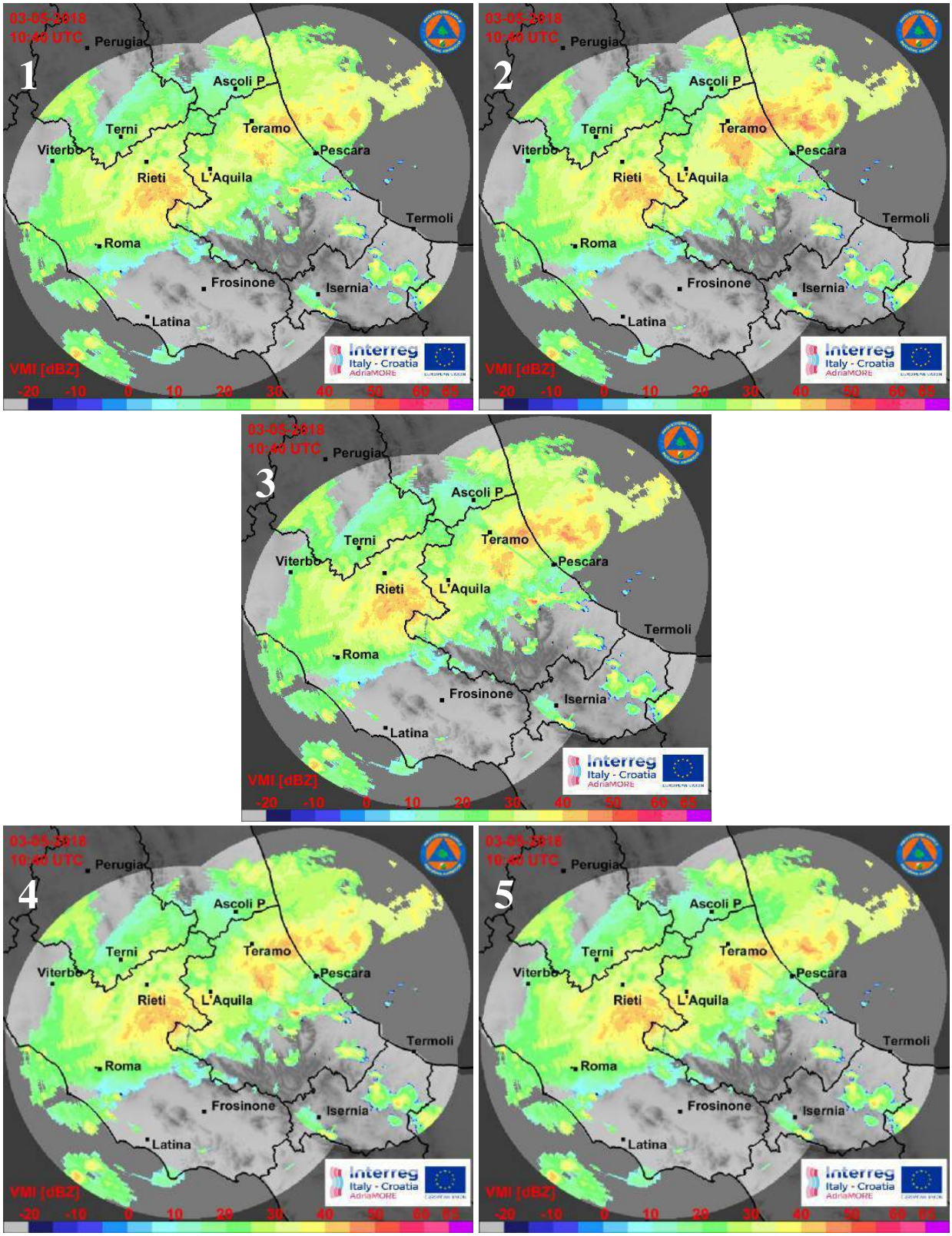

Figure 6.9a *Example of reflectivity composite techniques in the composite domain on May 3, 2018 at 10:40 UTC. MEAN reflectivity (1), MAXIMUM reflectivity (2), LINEAR WEIGHTED with the distance (3), EXPONENTIAL WEIGHTED with the distance (4) and INVERSE DISTANCE WEIGHTED (5)*

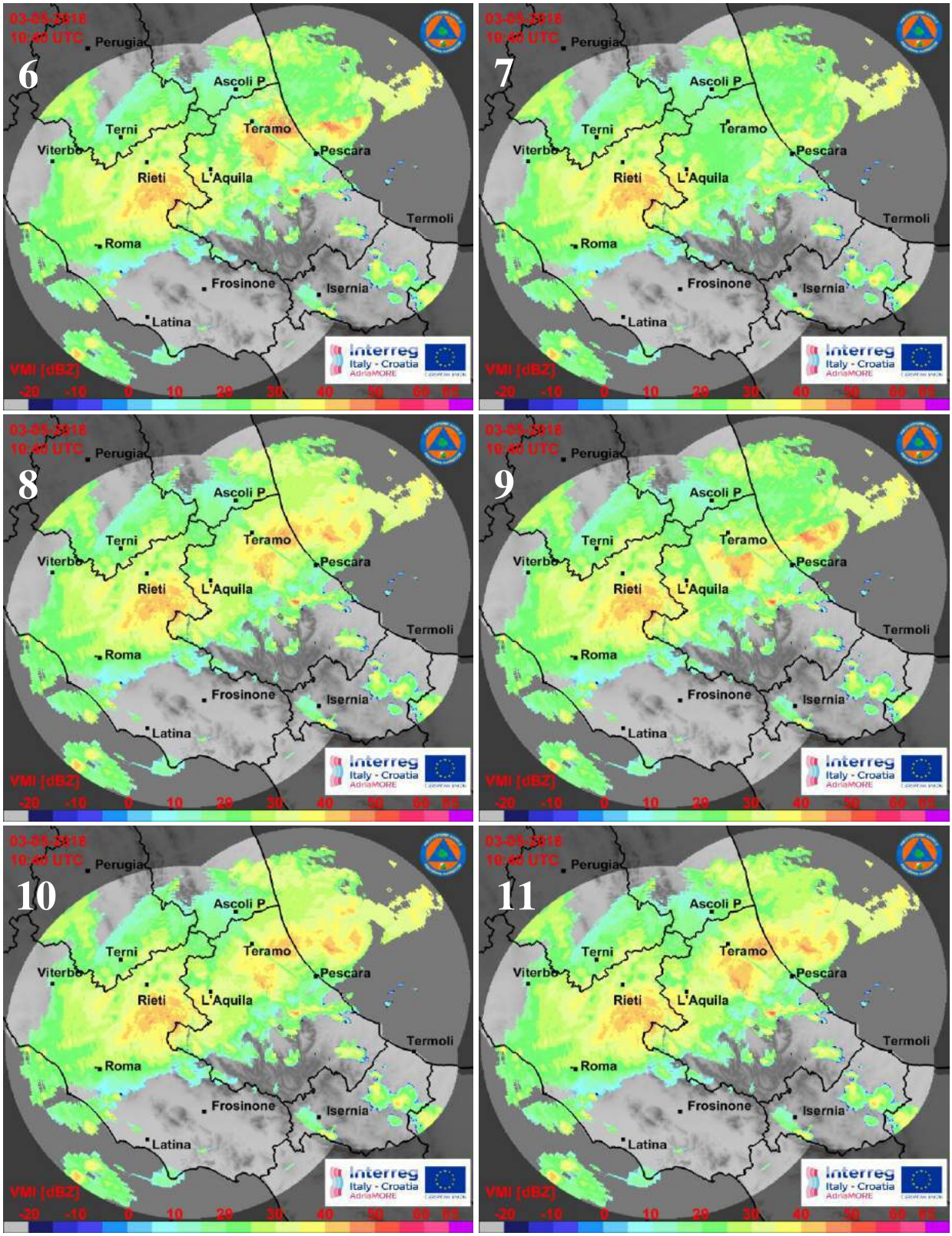

Figure 6.9b *Example of reflectivity composite techniques in the composite domain on May 3, 2018 at 10:40 UTC. MAXIMUM QUALITY (6), MINIMUM PIA (7), QUALITY WEIGHTED (8) and MINIMUM DISTANCE (9, QUADRATIC WEIGHTED with the distance (10) and QUALITY-DISTANCE WEIGHTED (11)*

6.3 Event occurred on June 8, 2018

The case study of June 8, 2018 was determined by an Atlantic perturbation that crossed central Italy in the previous hours (**figure 6.10**) characterized by a strong atmospheric instability that developed several phenomena with hail and storms on the eastern sectors of the Abruzzo region. From the rain gauges, some well-demarcated areas with peaks of 30-40 mm/24h are evident, mainly near the major reliefs (**figure 6.11).**

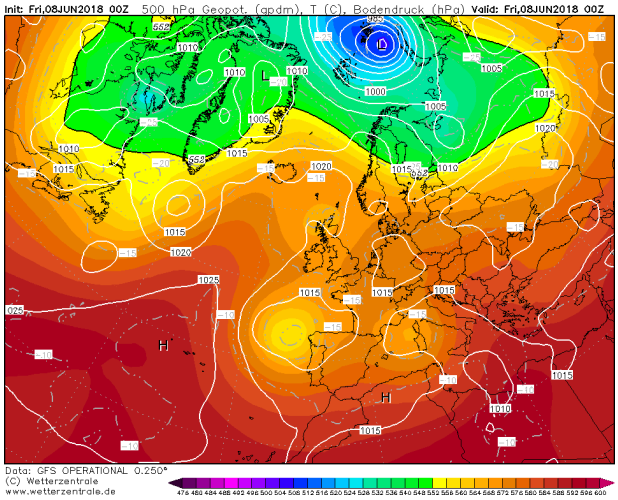

Figure 6.10 *GFS map of geopotential in gpdm at 500 hPa (shaded colors), temperature in ° C (dashed-point isolines in gray) and ground pressure in hPa (white isolines) at 00:00 UTC on June 8, 2018*

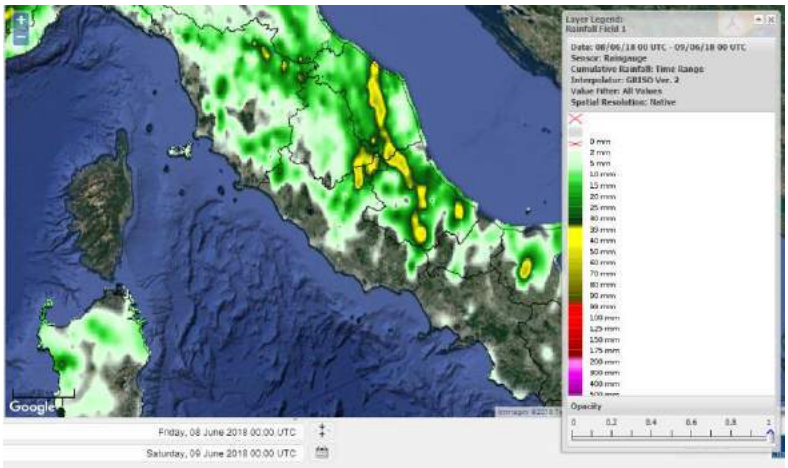

Figure 6.11 *Map of ground precipitation accumulated in 24 hours starting from 00:00 UTC on June 8, 2018 from the DEWETRA DPC rain gauges network [right panel]*

Among the present radars, the X-band systems have a better characterization of the precipitation cells along the Adriatic coast, but sometimes may have partial loss of reflectivity signal due to the greater attenuation of the X-band wavelength, compensated by C-band radars in the overlapped observation area.

In the **figure 6.12** are shown some examples of the composite radar products (SRI, CSD, VIL and POH) obtained with the Maximum Quality algorithm (method 6 of table 5.3). The maps are in-line with the convective characteristic of the precipitation that is locale high values of SRI and VIL as well as the presence of many convective areas in the CSD where a high POH values is associated.

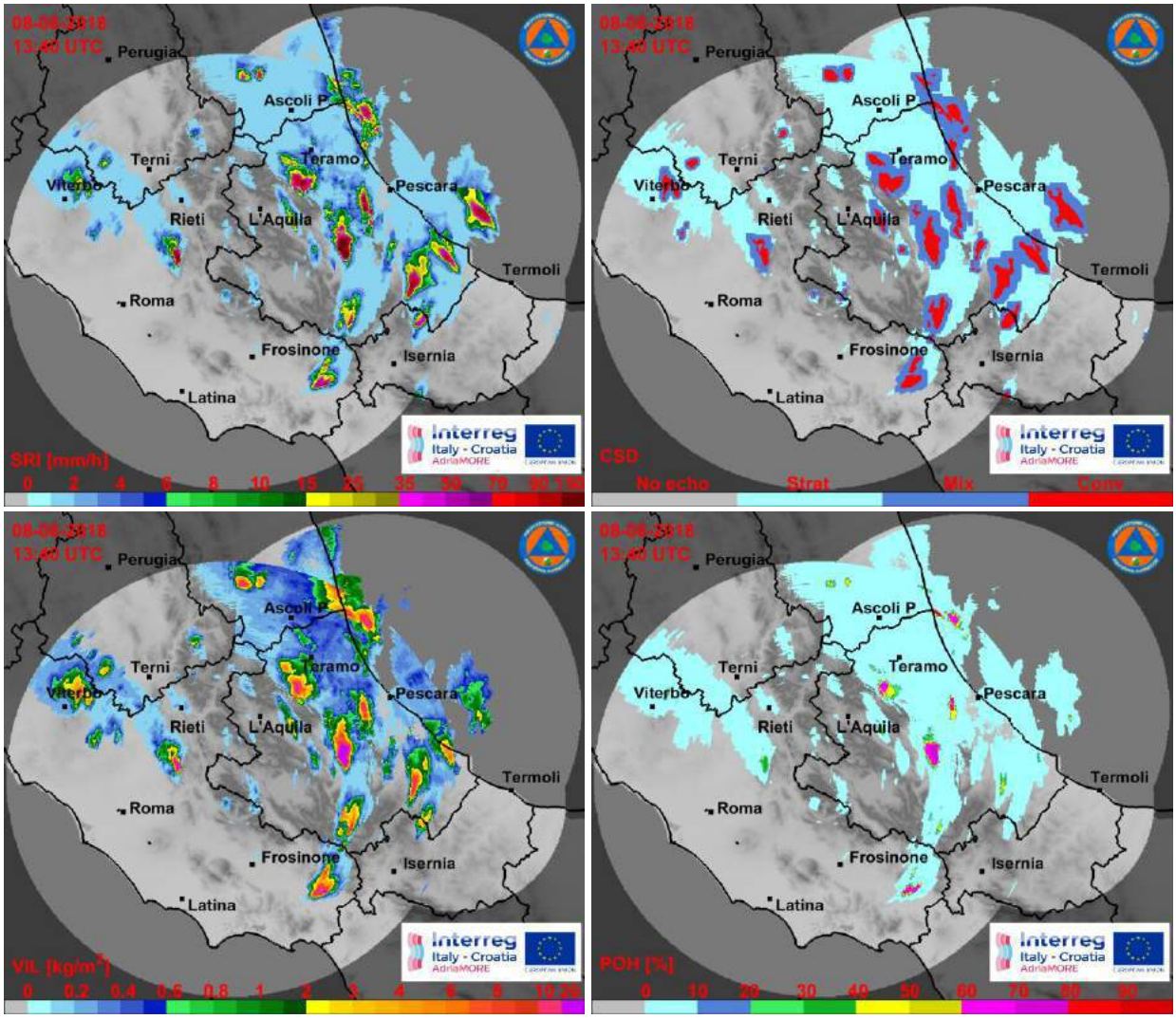

Figure 6.12 *Examples of composite radar products on June 8, 2018 at 13:40 UTC: SRI (top left), CSD (top right), VIL (bottom left) and POH (bottom right)*

Visual comparison of **figure 6.13a** and **figure 6.13b** panels shows discrepancies with respect to the different compositing techniques. The highest observed reflectivity values in convective cells are better reproduced in the panel 2 than in the other panels. Moreover, the mosaics obtained with Weighted Nearest-Radar methods (panels 3, 4, 5 and 10) are more similar to each other, in particular showing good representation of the convective cells in the overlapping areas. The panels 6 and 7 show a not good representation of the convective cells in the overlap area due to the effect of PIA which influences both the mosaicking methods since both methods use the minimum attenuation as quality indicator. For this reason, in case of strong attenuation, convective cells could be partially represented in the mosaic domain. This can be compensated by associating a further weight to the quality as shown in panel 11, where the combined action of quality and distance manages to overcome the limitations of the methods used individually. The method of weighted Quality (panel 8), since the weight is determined dynamically, i.e. based on the errors deteriorating data from single term of observation, is dynamic as well. The composite reflects this condition especially at longer distance where this method can cause underestimation.

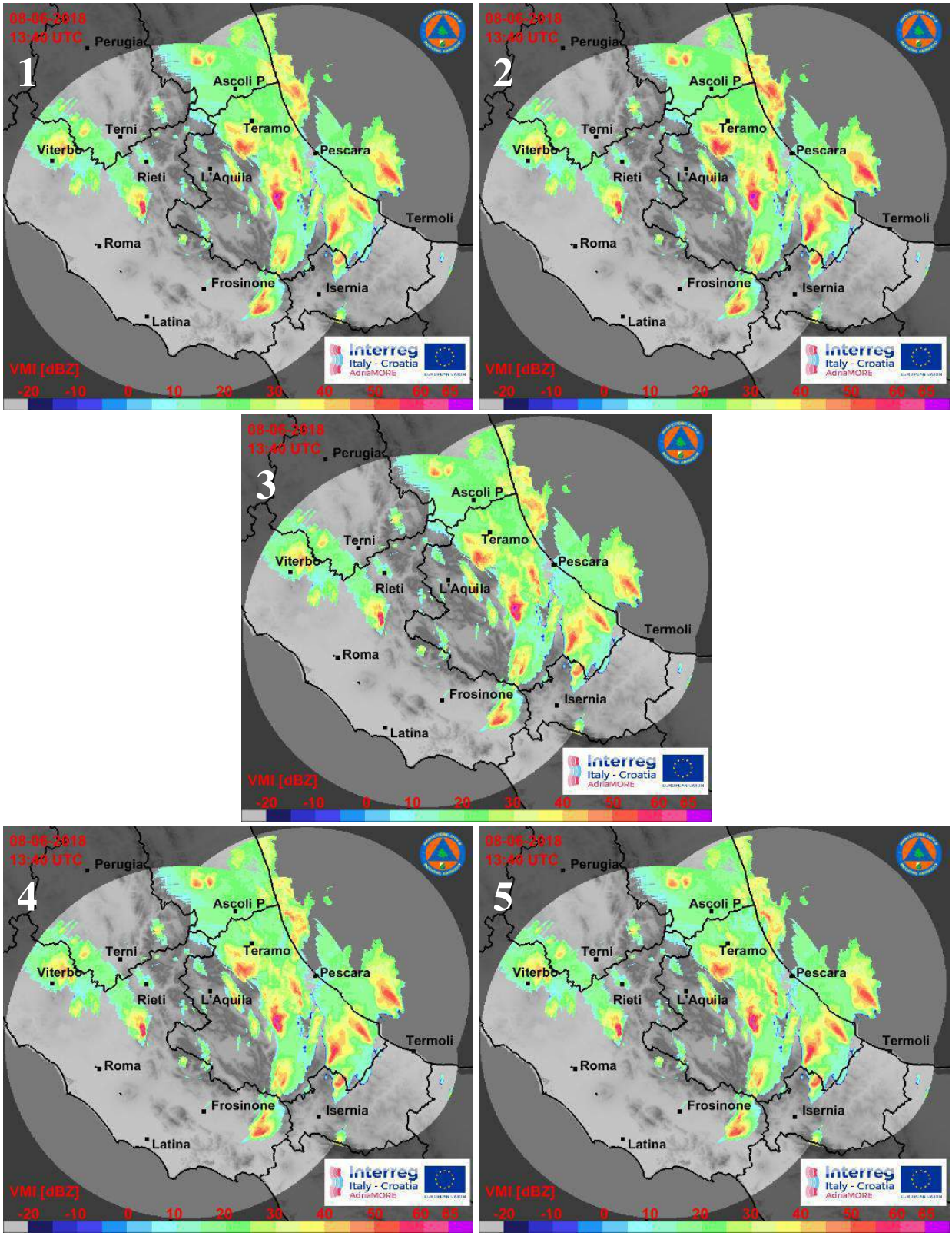

Figure 6.13a *Example of reflectivity composite techniques in the composite domain on June 8, 2018 at 13:40 UTC. MEAN reflectivity (1), MAXIMUM reflectivity (2), LINEAR WEIGHTED with the distance (3), EXPONENTIAL WEIGHTED with the distance (4) and INVERSE DISTANCE WEIGHTED (5)*

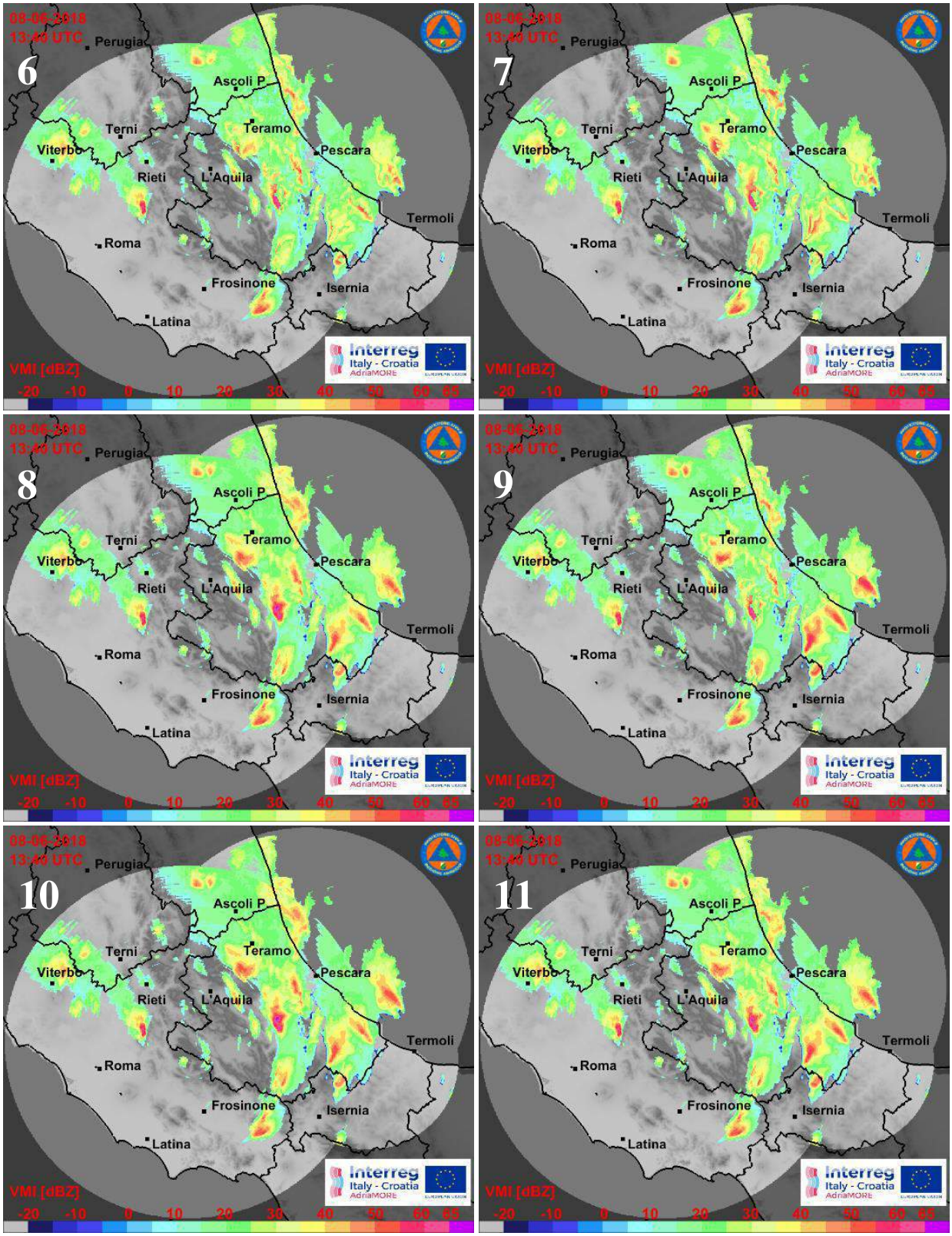

Figure 6.13b *Example of reflectivity composite techniques in the composite domain on June 8, 2018 at 13:40 UTC. MAXIMUM QUALITY (6), MINIMUM PIA (7), QUALITY WEIGHTED (8) and MINIMUM DISTANCE (9, QUADRATIC WEIGHTED with the distance (10) and QUALITY-DISTANCE WEIGHTED (11)*

6.4 Validation of mosaic methods by utilizing a rain gauge network

The mosaic composition methodology was evaluated, for May 3, 2018 case study, by comparing the precipitation estimates, obtained with the various mosaic techniques shown in table 5.3, with the relative measurements of rain gauges forming part of the Italian national network (**figure 6.14**).
In this analysis the whole day of May 3, 2018 was considered.

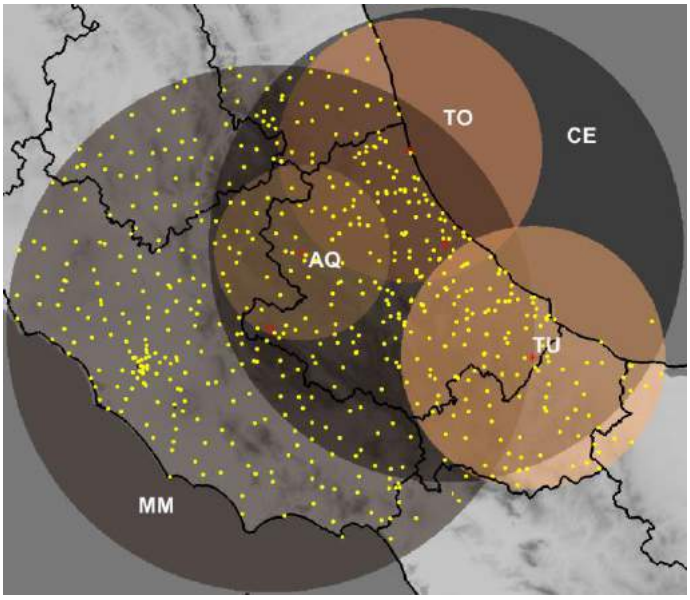

Figure 6.14 *Distribution of rain gauges available in the mosaic domain*

Acquisition and processing of rainfall data are performed by regional authorities at different time intervals, ranging from 5 to 30 min.
The data of the rain gauge network are collected through the telephone networks for communication (fixed-line or low-power cellular network) and the UHF/VHF radio link to be processed, centrally in near real time, by the Italian Department of Civil Protection (DPC). The set of one hour of rain accumulated for each rain gauge of the network represents the product of the intensity of the rain (G, mm/h). The DPC distributes products related to instantaneous precipitation and accumulated through DEWETRA, a customized web-based software.
Quality control of rain gauges measurement data is the first step in the context of an operational use of the data.
Therefore, the rainfall data are preliminarily subjected to a quality control in order to identify and remove any inconsistencies. The quality control carried out includes the following actions:

1) control of rain gauges with the same name but different coordinates;
2) removal of data associated with rain gauges without valid coordinates;
3) removal of duplicate data;
4) control of the same rain gauges with different values at the same time;
5) control of rain gauges with an instantaneous precipitation rate too high;
6) identification of anomalous data (for example very different values respect to the surrounding rain gauges).

A network of 659 rain gauges are present in the coverage area of the mosaic domain and their data are available every hour (hourly cumulated precipitation. All the above error sources have been corrected and for this analysis only high-quality rain gauges have been taken into account, in fact after the correction procedure of the measurement errors it is assumed that the remaining errors are negligible compared to the radar bias. Among all the rain gauges available only slightly more than 6% were not used in this analysis (**figure 6.15**).

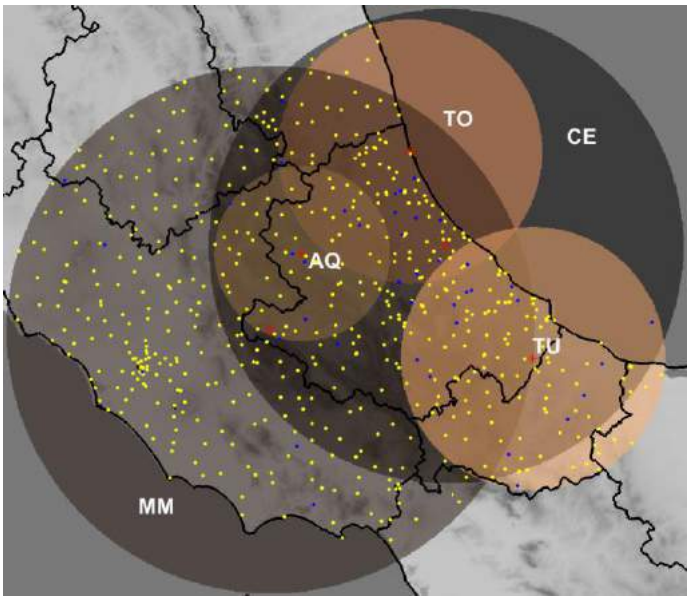

Figure 6.15 *Distribution of rain gauges in the mosaic domain in which only one part (in blue) did not pass the quality control*

In order to compare cumulated hourly of the rain gauges with the precipitation estimates by the various radar mosaic techniques, the SRT composite product at an hour was taken into account and indicated, for simplicity, with the symbol R. Moreover, precipitation values lower than 0.2 mm measured from the radar are to be considered null because the rain gauges used cannot measure values lower than this threshold.

To compare the radar estimates and the rain gauges, it is necessary to combine the position of the rain gauge with the corresponding radar cell. Due to the resolution of the domain and the areal measurement of the radar compared to the punctual one of the rain gauge, an uncertainty is introduced on the match between radar cell and rain gauge position.

Since the variability of precipitation fields strongly depends on the way in which the spatial coupling between radar and rain gauges is considered, a meaningful comparison is not trivial. For this reason, around the cell of the radar domain, corresponding to the rain gauge position, the neighboring cells were also used in order to create a 3x3, grid whose radar data, contained therein, are used in different modes of spatial coupling:

a) **Nv** (Nearest value). The value within the grid closest to the value of the rain gauge.
b) **Mean**. The mean value between the internal values of the grid.
c) **Max.** The maximum between the values in the grid.
d) **Median**. The value that separates the upper half of the internal values of the grid, from the lower half.

The quality of the comparison is assessed using the following indicators. The absolute error (ERR) is defined as the difference between the estimates of the hourly precipitation from the radar (R) with the relative hourly data measured by the rain gauges indicated with G:

$$ERR = R - G \tag{6.1}$$

By indicating the mean with respect to time with angle brackets, we introduce the following statistical indicators:
Mean error or ***BIAS*** ranging from 0 to ∞ *(optimal value 0)*:

$$BIAS = \langle ERR \rangle \tag{6.2}$$

Mean-Field Ratio Bias (***MRB***) ranging from -∞ to ∞ *(optimal value 1)*:

$$MRB = \frac{\langle R \rangle}{\langle G \rangle} \tag{6.3}$$

Mean Absolute Error (***MAE***) ranging from 0 to ∞ *(optimal value 0)*:

$$MAE = \langle |ERR| \rangle \tag{6.4}$$

Root Mean Square Error (***RMSE***) ranging from 0 to ∞ *(optimal value 0)*:

$$RMSE = \sqrt{\langle (ERR)^2 \rangle} \tag{6.5}$$

Fractional Standard Error (***FSE***) ranging from 0 to ∞ *(optimal value 0)*:

$$FSE = \frac{\sqrt{\langle (ERR)^2 \rangle}}{\langle G \rangle} \tag{6.6}$$

Correlation Coefficient (***Corr***) ranging from -1 to 1 *(optimal value 1)*:

$$Corr = \frac{\langle (R - \langle R \rangle)\rangle\langle (G - \langle G \rangle)\rangle}{\sigma_R \cdot \sigma_G} \tag{6.7}$$

where σ_R e σ_G indicate, respectively, the standard deviation of radar observations and of rain gauges, defined as:

$$\sigma_R = \sqrt{\langle (R - \langle R \rangle)^2 \rangle} \qquad \sigma_G = \sqrt{\langle (G - \langle G \rangle)^2 \rangle} \tag{6.8}$$

Only a part of the eleven mosaic composition methods, introduced in table 5.3, have been analyzed as summarized in **table 6.1.** They are: the method of Mean (Mean), of Maximum (Max), the methods that use a weight Linearly (linDW), Exponentially (expDW) and Quadratically (quadDW) dependent on distance, the method of Maximum Quality (MaxQ), the method that uses a weight dependent on Quality (QW) and finally the method in which the weight function depends on Quality and distance (QDW).

Num.	Mosaicking method	Symbols
1	**Assign to the common pixel the mean value of the available measurements**	**Mean**
2	**Assign to the common pixel the maximum value of the available measurements**	**Max**
3	**Assign to the common pixel a value weighted with the distance from the radars, using linear weighting functions**	**linDW**
4	**Assign to the common pixel a value weighted with the distance from the radars, using exponential weighting functions**	**expDW**
5	Assign to the common pixel a value weighted by a defined inversely proportional power of the distance from the radar	not analyzed
6	**Assign to the common pixel the value corresponding to the maximum final quality (TQI)**	**MaxQ**
7	Assign to the common pixel the value corresponding to the minimum PIA (Path Integrated Attenuation)	not analyzed
8	**Assign to the common pixel a value weighed by the final quality (TQI) associated with the various radars**	**QW**
9	Assign to the common pixel the value corresponding to the minimum distance	not analyzed
10	**Assign to the common pixel a value weighed quadratically with the distance from the radar**	**quadDW**
11	**Assign to the common pixel a value weighted with the final quality (TQI) and a defined inversely proportional power of the distance from the radar**	**QDW**

Table 6.1 *In bold, the mosaic methods analyzed with the respective symbols used in the graphs*

Figure 6.16 shows the main statistical indicators (Corr, Bias, RMSE and FME) associated with the radar-gauge coupling mode (Nv, Mean, Max, Median) and for each of the mosaic techniques examined highlighted in table 6.1. Each curve it represents the way in which the rain estimate of the radar has been associated to the rain gauge, while in abscissa are indicated the methods for mosaicking.

For each index shown, associating the radar data with the rain gauge data using the "nearest value" (Nv) method ensures the best performance. The other modalities (indicated in the legend) have lower values, and this leads to the choice to continue the analysis using exclusively the Nv procedure.

With the same spatial coupling method used, the mosaic composition technique with the best scores is the highest quality (maxQ).

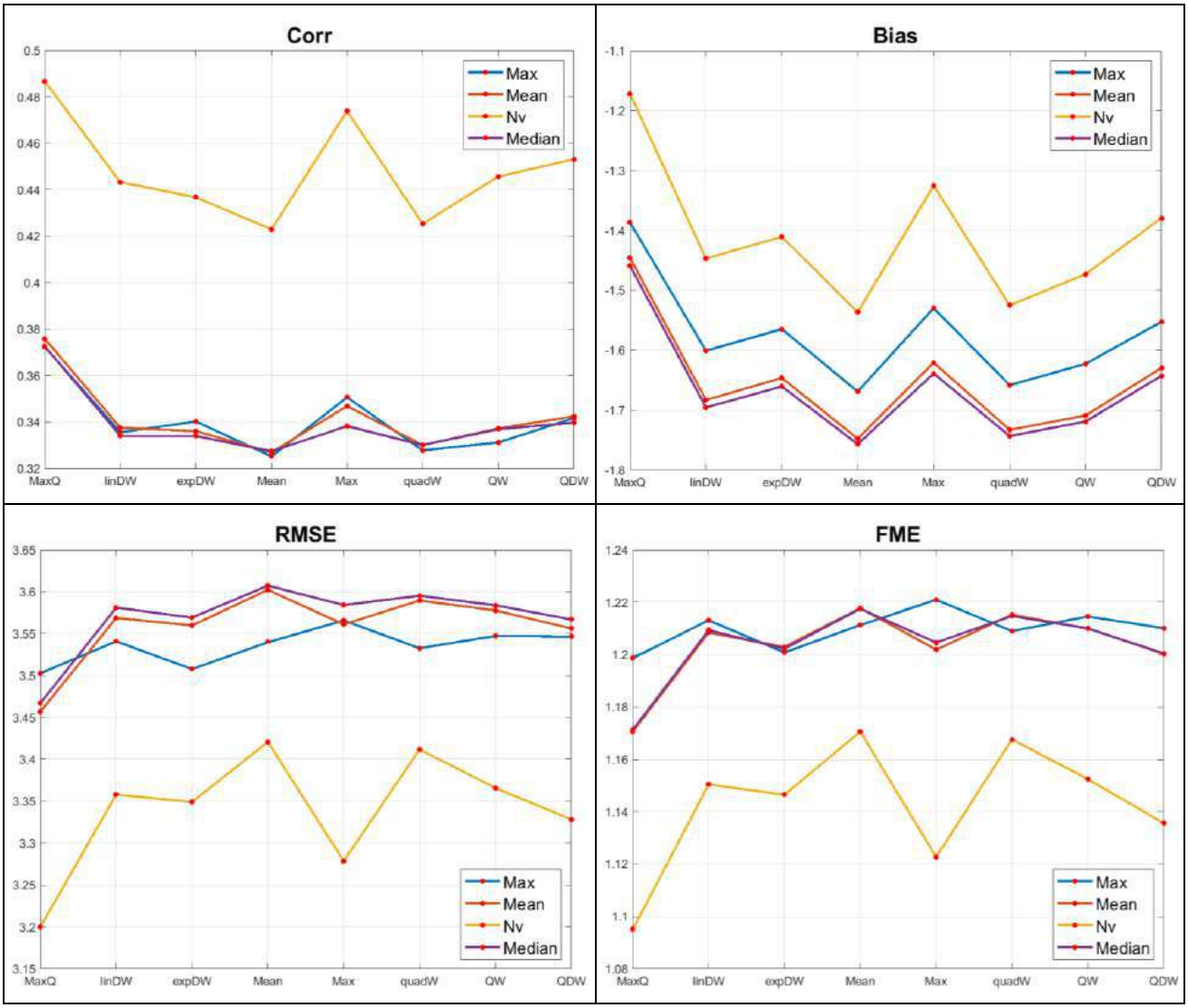

Figure 6.16 *Statistical indicators of Correlation (top left), Bias (top right), RMSE (bottom left) and FME (bottom right) related to the spatial coupling and mosaic composition method*

Note that the Bias graph shows negative values for all the mosaic methods, indicating a general underestimation of the radar with respect to the rain gauge. This is also observable in scatter plots of **figures 6.17** and **6.18** which show the cumulated hourly of radar estimates with respect to rainfall measurements. The color of the graph changes according to the density of the number of occurrences of the pairs (G, R), while the red line represents the linear regression curve with the best correspondence between radar measurements and rain gauges.

All the analyzed methods show a general underestimation of the radar measurements compared to those detected by the rain gauges, visible from the regression line (red) that appears below the bisecting line (black).

Finally, **table 6.2** summarizes the scores of statistical indicators related to the different mosaic methodologies, using the radar-gauge spatial coupling method of the Nearest value. The highest quality (MaxQ in green) is the method that has obtained the best performance, while the average (MEAN, in red), is the technique whose estimates have diverged more from what is detected by rain gauge network.

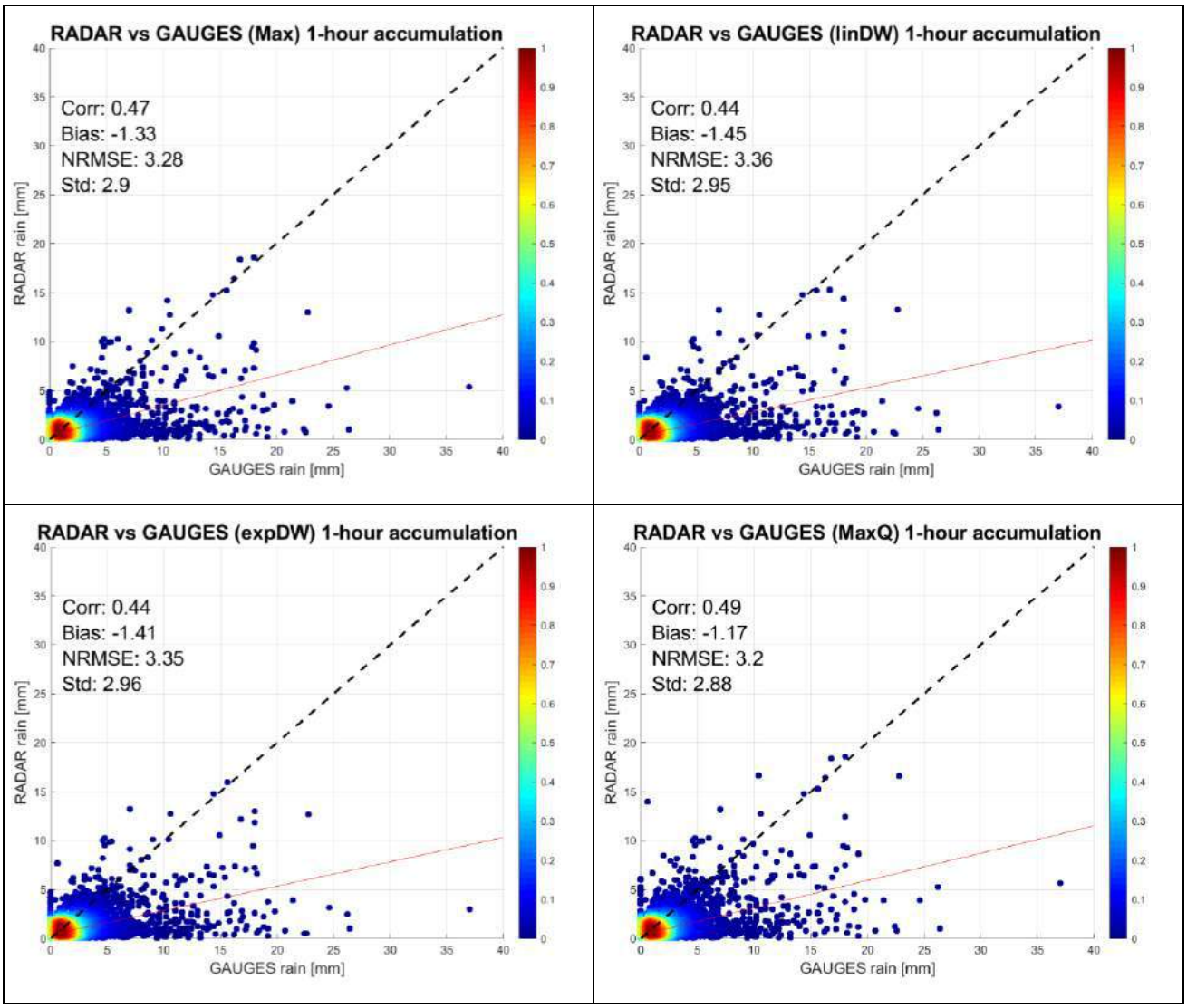

Figure 6.17 *Scatterplots of the hourly cumulated of May 3, 2018 for the methods of Maximum (Max), Linear Weight (linDW), Exponential Weight (expDW) and Maximum Quality (MaxQ)*

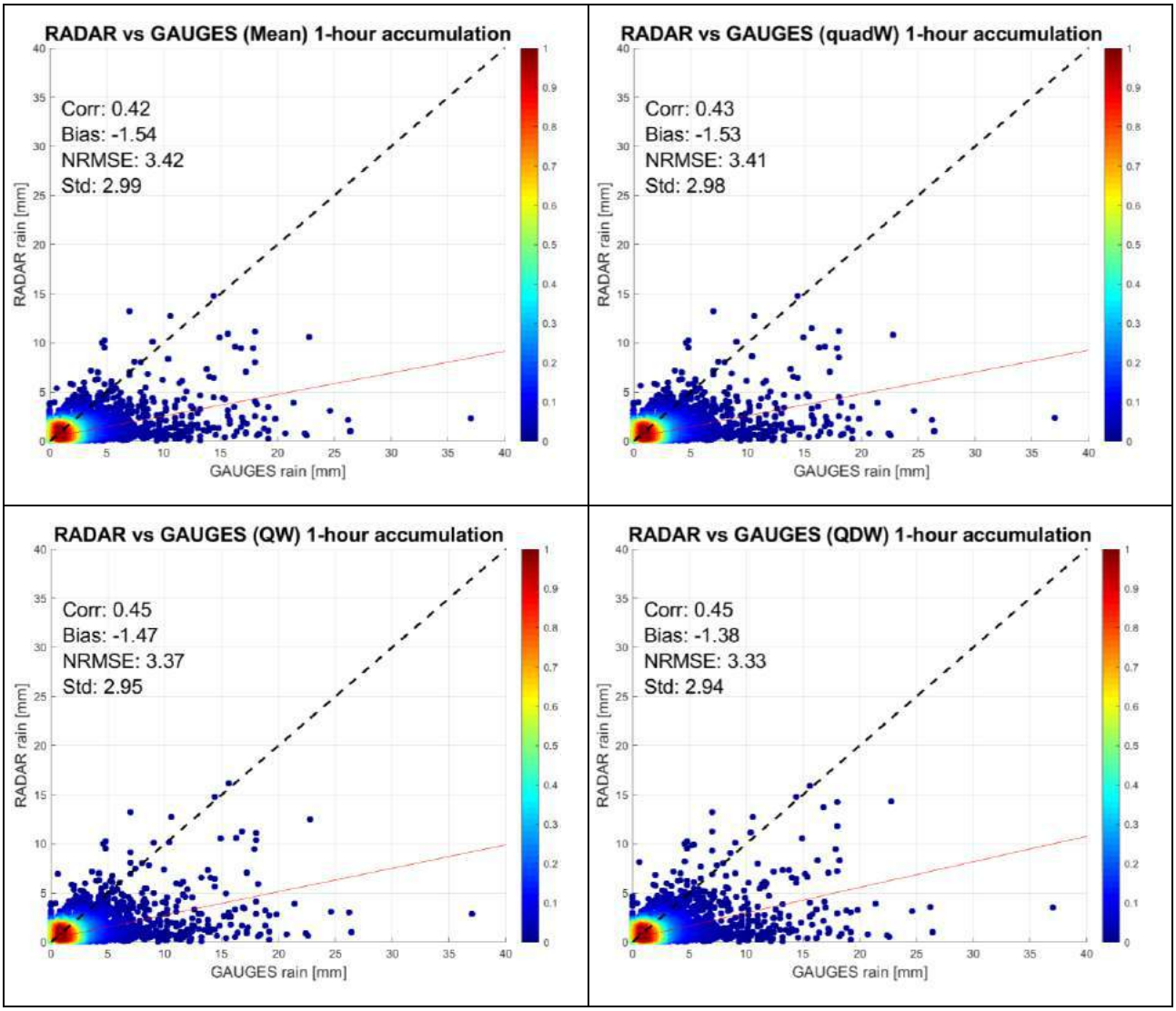

Figure 6.18 *Scatter plot of the hourly cumulated of May 3, 2018 for the methods of Mean (Mean), Quadratic Weight (quadW), Quality Weighing (QW), and Weight Quality + distance (QDW)*

	MaxQ	MEAN	linDW	expDW	MAX	quadW	QW	QDW
CORR	0,49	0,42	0,44	0,44	0,47	0,43	0,45	0,45
BIAS	-1,17	-1,54	-1,45	-1,41	-1,33	-1,53	-1,47	-1,38
STD	2,88	2,99	2,95	2,96	2,90	2,98	2,95	2,94
MAE	1,71	1,86	1,82	1,81	1,77	1,86	1,82	1,80
RMSE	3,20	3,42	3,36	3,35	3,28	3,41	3,37	3,33
FSE	1,10	1,17	1,15	1,15	1,12	1,17	1,15	1,14

Table 6.2 *Error indexes calculated for hourly cumulated related to the mosaic composition techniques for the event of May 3, 2018. In green and red respectively the technique with the best and worst performance*

7. SUMMARY AND OUTLOOK

Weather radars are ideally suited to provide remotely sensed data of the state of the atmosphere over a wide geographic area. The data provided by weather radars are often used for the near real-time forecasting of weather events by meteorologists, but can also be used to initialize numerical weather predictions, provide and hydrological models. Given the wide uses of data from weather radar, it is not surprising that there has been considerable investment in the development and operation of these instruments worldwide. Networks of radars cover much of the inhabited regions of North America and Europe, providing updated views for severe weather detection and mesoscale flood forecasting. Nonetheless measurements made by weather radars contain a tremendous amount of information, yet considerable effort must be made to extract out scientifically and operationally meaningful products. Processing, correcting and analysing weather radar data covers a wide range of computational disciplines and fields. Given the wide scope of information that weather radars can provide, having flexible and extendable software to process their data is key.

Moreover, selecting an optimal way to merge radar data from different systems is significant and must consider a number of factors such as the size and shape of the domain of interest, number and location of the network's nodes. In practice, operating a network of several radars (nodes) as a single instrument means that information from individual radars is shared in data post-processing. In this case, the quality of the final rainfall products varies depending on how many nodes are used, how radar data are merged, and what quality control steps are implemented.

This deliverable described the weather radar network software which has been developed in the framework of AdriaMORE project. It is able to ingest and process data from systems with different features for the creation of a radar composite products. This software, called CRAMS (Cetemps Radar Advanced Mosaic Software) can ingest as input both 3D raw volumes and 2D products data and gives as main output (1) 2D products focused on extreme events for each individual radar and (2) composite radar products for weather monitoring (**figure 7.1**).

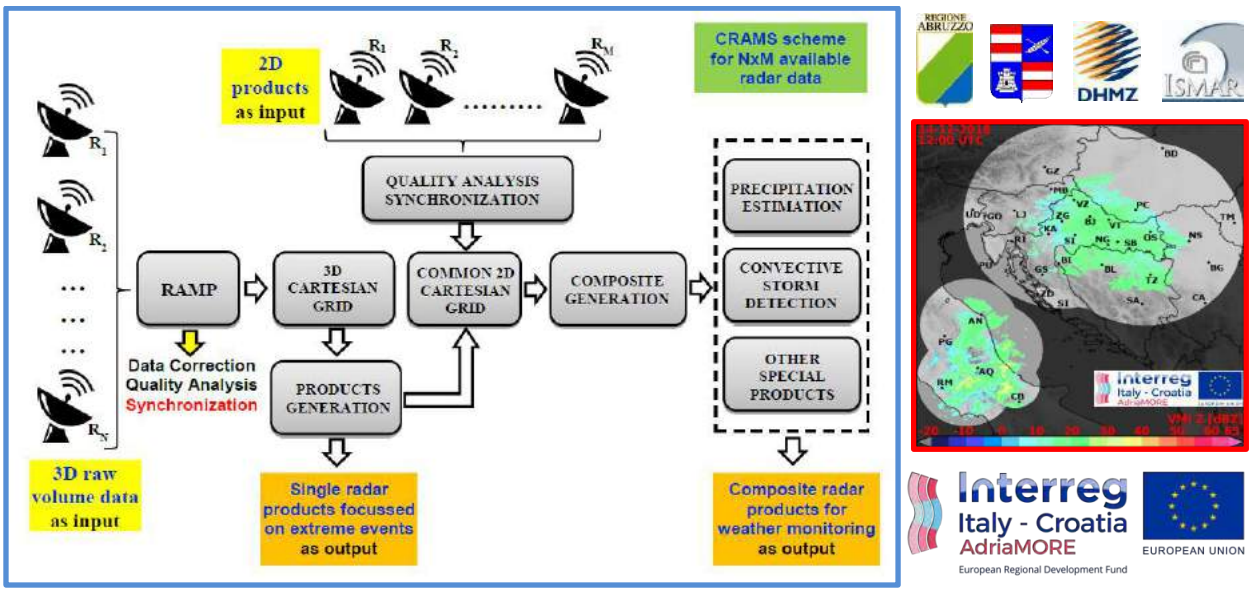

Figure 7.1 *Block diagram of the Cetemps Radar Advanced Mosaic Software (CRAMS) developed within the AdriaMORE project*

All algorithms have been developed by using Python programming language, CRAMS.py software is a Python package that provides a variety of routines for reading, processing, analysing, compositing and visualizing data from different weather radars.
The package is organized in a number of sub-packages (modules) roughly separated by the type of functionality they provide. It is designed to provide the tools required for building complete radar processing chains in a flexible way in order to be adapted for different radar network.

CRAMS has been tested by utilizing Italian and Croatian radars, the composite domain was defined taking into account the technical characteristics of the radars, their geographical location and the peculiarities of the concerned territory.
In the CRAMS a suitable pre-processing chain has been implemented (which utilizing single and dual polarization radar data at S-, C- and X bands as input) to eliminating, compensating or at least to identifying the most common error sources for different radar systems. Although it is not possible to make all radar systems to be mosaicking identical, it is possible to ensure harmonized technical and software platforms on which each radar data can be processed. The employed algorithms are functionally divided into two paths: one for data corrections and the second for data quality characterization. Particular quality algorithms can be switched on or off in the scheme. Processing by means of data correction algorithms allows the reduction of uncertainty in the data, whereas quality characterization algorithms generate a map of total quality index that can be attached to the data.

In this work, several peer reviewed article, proceeding and thesis on radar composite techniques have been fully analysed and eleven methods chosen. The assessment of the different merging methods on radar data has been conducted, on cases studies in diverse storm regimes, by using the Abruzzo Region radar network. Preliminary results were shown at the ERAD (European Conference on Radar in Meteorology and Hydrology) conference, held in Holland in July 2018. We emphasize that how the principle of Maximum Quality (method 6 in table 5.3) is a good compromise between the tested methods since it is comprehensive of the major problems affecting radar data.
Moreover, since several meteorological services across the world are using networks of weather surveillance radars, a review of the main network have been conducted, especially with respect to the systems operating at X-band frequencies which have been tested during several EU-funded or National projects focused on operational systems.

As mentioned before, CRAMS has been tested on Abruzzo and Croatian network but it was built in a flexible way and can be applied to the larger domain including other radar systems.
As an example, for Italian side, in **figure 7.2** are shown some composite products obtained including Cingoli radar at the Abruzzo network. Cingoli radar, managed by the Functional Centre of Marche Region, has been operational again since November 2018 thus we could not use it for a fully analysis of CRAMS.
In the framework of dissemination activities, we discuss with the manager of the two X-band radar installed in the Campania region (in Napoli and Trevico) in order to extend the mosaic coverage.

Find in the **figure7.3** the currently domain of Abruzzo network, the domain which includes Cingoli radar and the domain which includes Napoli and Trevico radars.

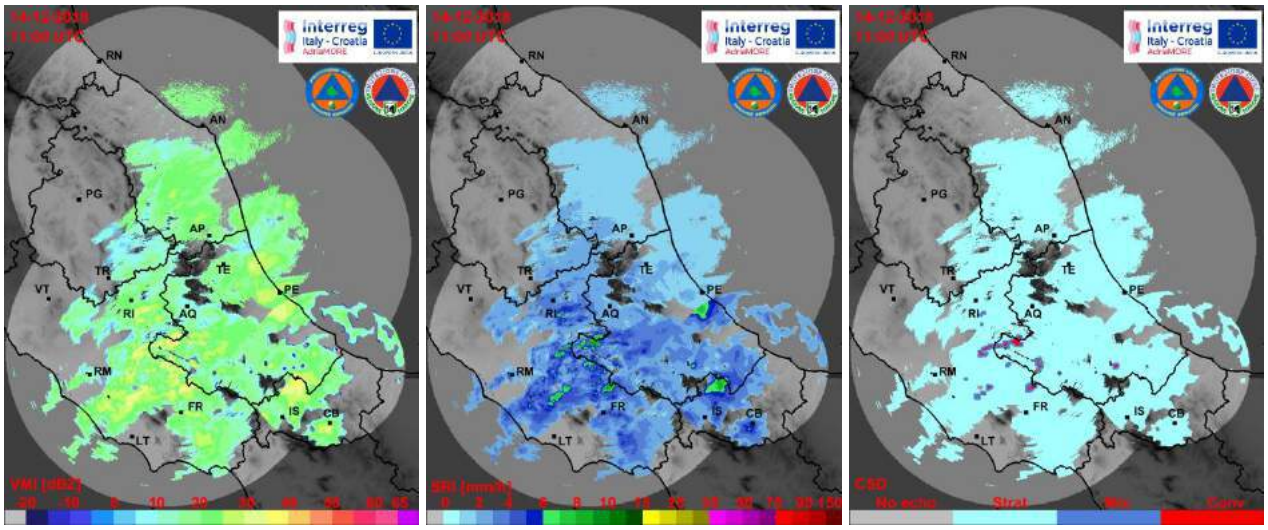

Figure 7.2 *Composite products including Cingoli radar in the Abruzzo network: VMI (left panel) SRI (central panel) and CSD (right panel) taken on December 14, 2018 at 11:00 UTC*

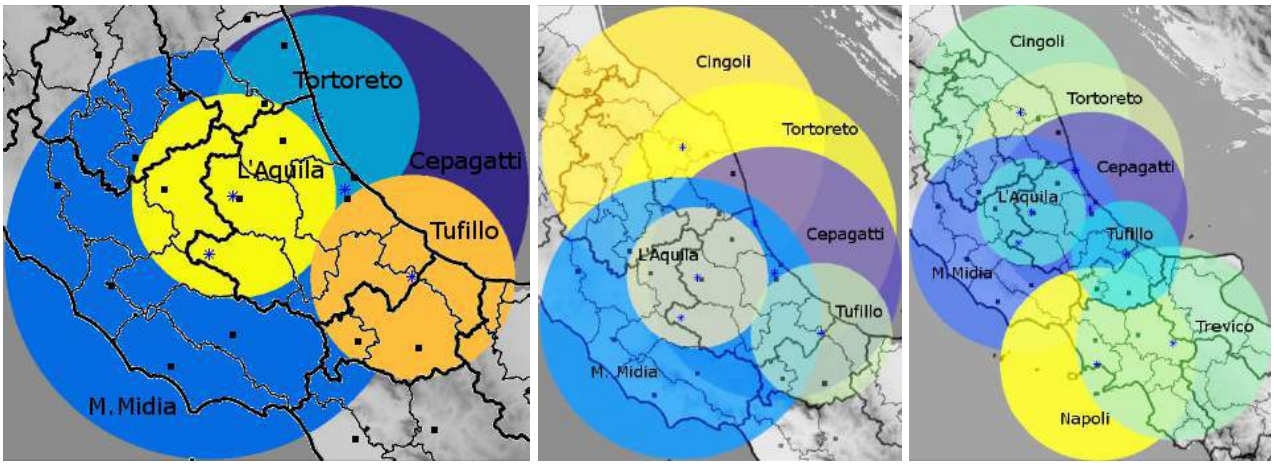

Figure 7.3 *Composite domain including in the Abruzzo network (left panel) Cingoli radar (central panel) and Napoli and Trevico radars (right panel)*

For Croatian side, as described in chapter 4, the radar network is currently constituted by three S-band systems, installed inland (**figure 7.4, left panel**), leaving the Adriatic coastline basically uncovered. In the next year thanks to the METMONIC project, started on November 2017, the existing three S-band weather radars are going to be replaced with new weather radars and three new radars are going to be placed along the Adriatic coast (**figure 7.4, right panel**). These radars are and will be managed by the Meteorological and Hydrological Service of Croatia partner of AdriaMORE project.

The network will be completed by Dubrovnik radar, installed during AdriaRadNet project (see chapter 3), once it will be operative again. The radar is currently under maintenance due to hardware problems, it is managed by the Dubrovnik Neretva Region, partner of the AdriaMORE project.

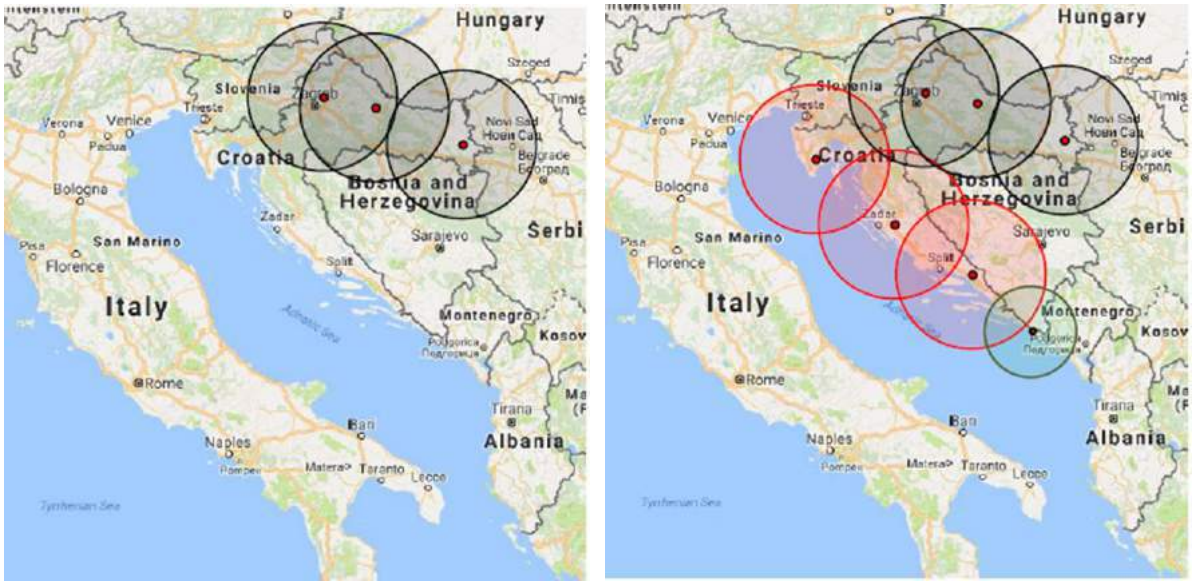

Figure 7.4 *Currently Croatian radar network (left panel) and those planned in the framework of METMONIC project (right panel). Red circles indicate the coverage of the new installations along the Adriatic coastline while green circle the coverage of Dubrovnik radar*

Once the three radars have been installed on the Croatian coastline, it will make sense to create a unique composite by overlapping the Italian and Croatian radars using the CRAMS chain.
In the **left panel of figure 7.5** is shown the planned unique composite by using the Italian radars currently available while in the **right panel of figure 7.5** the planned unique composite by adding the available radars in the north of Italy in order to cover the northern part of the Adriatic Sea.

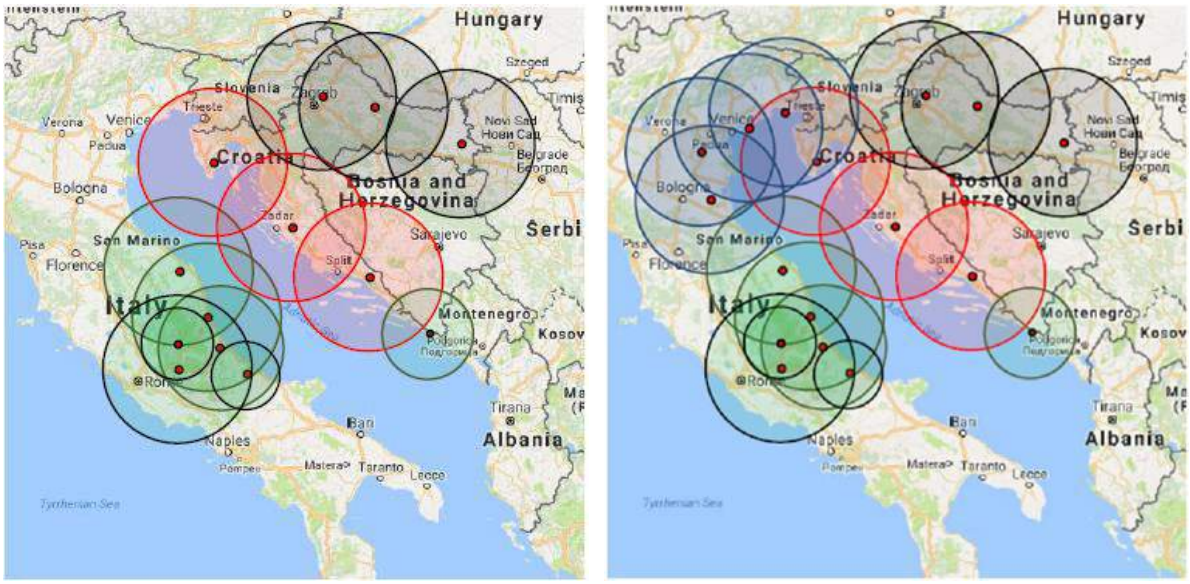

Figure 7.5 *Adriatic composite utilizing the Croatian radar planned in the framework of METMONIC project and the Italian radar used in this work (left panel) and by adding the available radars in the north of Italy (right panel)*

Finally, an example of unique composite map, by utilizing Croatian and Italian radars currently available, is shown in **figure 7.6** for the event of December 14, 2018 at 12:00 UTC. For completeness, in **figure 7.7** are shown the composite maps in Italian and Croatian domains for the same event at the same time.

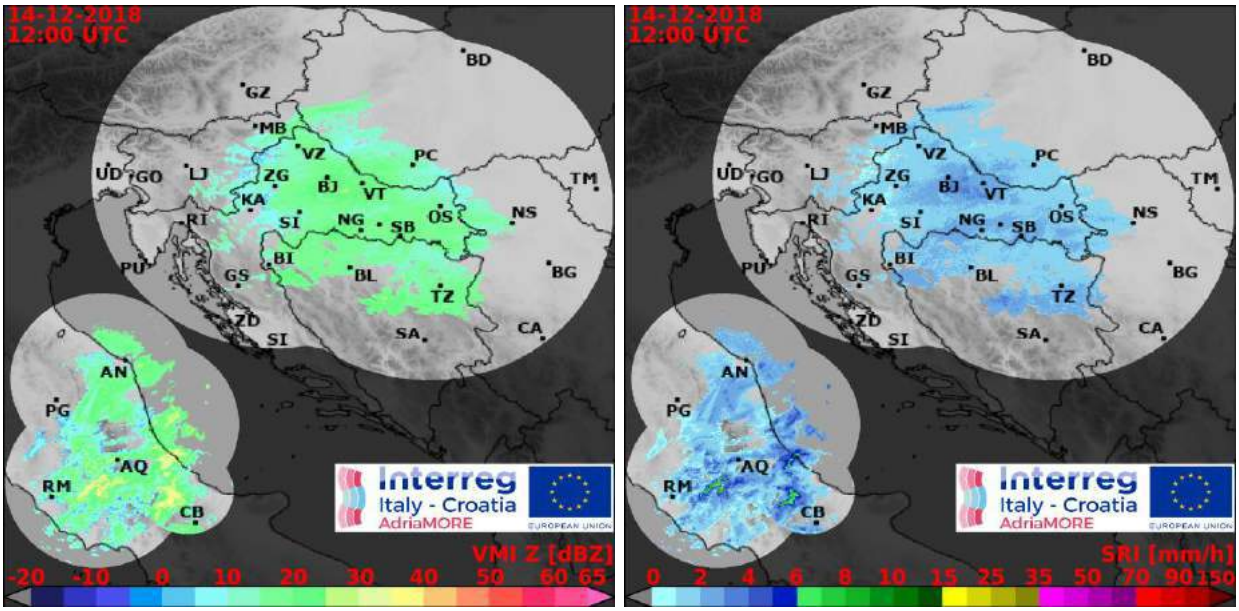

Figure 7.6 *Unique composite taken on December 14, 2018 at 12:00 UTC by utilizing Croatian and Italian radars currently available. In the left panel is shown the VMI product while in the right panel the SRI product*

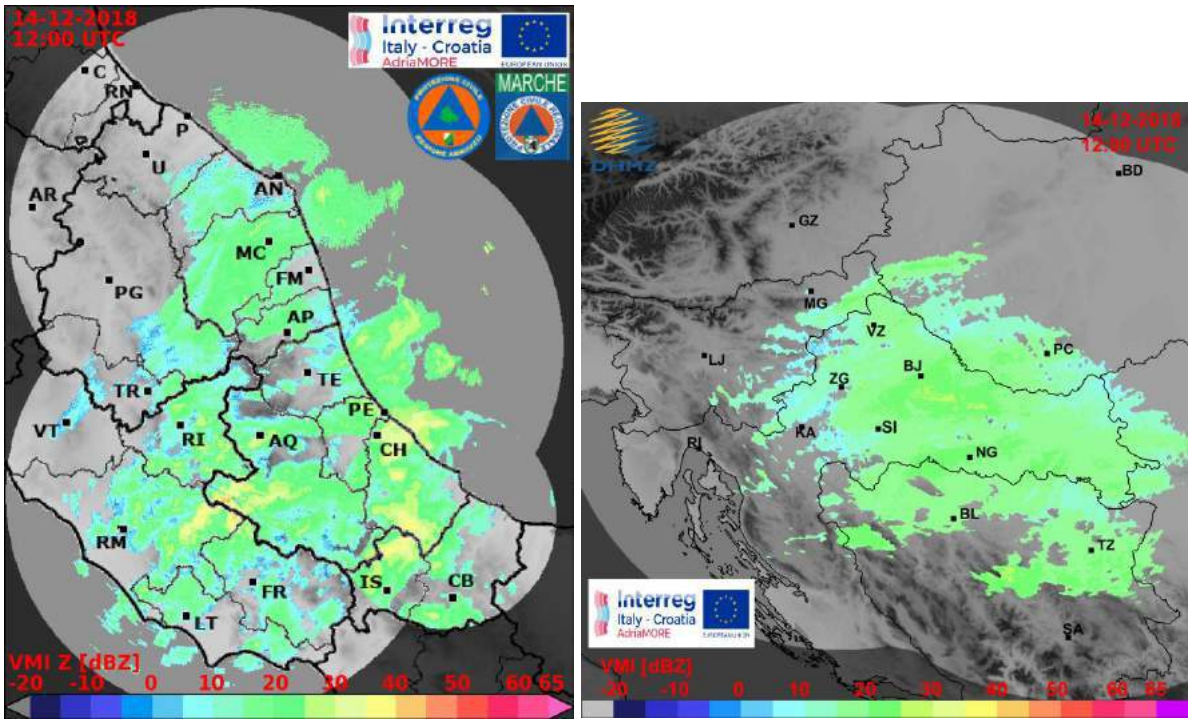

Figure 7.7 *Same composites of the VMI product of figure 7.6 in the Italian (left panel) and Croatian (right panel) domains*

8. REFERENCES

- **Antonini, A**. et al. "On the Implementation of a Regional X-Band Weather Radar Network" Atmosphere year 2017, 8, 25; doi:10.3390/atmos8020025, **2017**
- **Barbieri, S**. "Testing of dual-polarization processing algorithms for radar rainfall estimation in tropical scenarios", HSAF, Visiting Scientist H_AS17_01 report, **2017**
- **Barbieri, S.,** Picciotti, E., Montopoli, M., Di Fabio, S., Lidori, R., Marzano, F. S., Kalogiros, J., Anagnostou M. and Baldini L., " Intercomparison of dual-polarization X-band miniradar performances with reference radar systems at X and C band in Rome supersite" Proc. ERAD2014, Garmisch-Partenkirchen (Germany), 1-5 September **2014**
- **Battan, L. J.** "Radar observation of the atmosphere", University of Chicago Press, ISBN 9780226039190, Chicago – London, UK, **1973**
- **Bebbington, D**.; Rae, S., Bech, J., Codina, B. and Picanyol, M. "Modelling of weather radar echoes from anomalous propagation using a hybrid parabolic equation method and NWP model data", Natural Hazards and Earth System Sciences, Vol. 7, pp. 391–398, ISSN 1561-8633, **2007**
- **Bech, J.**, Codina, B., Lorente J. and Bebbington D. "The sensitivity of single polarization weather radar beam blockage correction to variability in the vertical refractivity gradient", J. Atmos. Oc. Tech., vol. 20, pp. 845-855, **2003**
- **Bertoldo** et al. "An Operative X-band Mini-radar network to Monitor Rainfall Events with High Time and Space Resolution", ETASR - Engineering, Technology & Applied Science Research Vol. 2, _246-250, **2012**
- **Bringi, V.N.** and Chandrasekar, V. "Polarimetric Doppler Weather Radar: Principles and Applications", Cambridge, UK, Cambridge University Press, **2001**
- **Charba J.** and Liang F. "Quality control of gridded national radar reflectivity data" in 21st Conf. on Wea. Analysis and Forecasting/17th Conf. on Numerical Wea. Prediction, (Washington, DC), p. 6A.5, Aug. **2005**
- **Collier, C. G**. "Applications of weather radar systems", A guide to uses of radar data in meteorology and hydrology. Wiley-Praxis, ISBN 0-7458-0510-8, Chichester, UK, **1996**
- **Domaszczynski, P.** "Performance evaluation of a network of polarimetric X-Band radars used for rainfall estimation." PhD diss., University of Iowa, **2012**
- **Doviak, R. J.** and Zrnic, D. S. "Doppler Radar and Weather Observations", Academic Press, **1993**
- **Einfalt, T.**, Lobbrecht, A., Leung, K. and Lempio, G. "Preparation and evaluation of a Dutch-German radar composite to enhance precipitation information in border areas", Journal of Hydrologic Engineering, Vol. 18 Issue 2, **2012**
- **Einfalt, T.** and Michaelides, S. "Quality control of precipitation data", In: Precipitation: Advances in measurement, estimation and prediction, S. Michaelides, (Ed.), 101–126, Springer-Verlag, Berlin – Heidelberg, Germany, **2008**
- **Fornasiero, A.**, Alberoni P. P., Amorati R. and Marsigli C. "Improving the radar data mosaicking procedure by means of a quality descriptor." In ERAD Publication Series, volume 3, pp. 378–341, **2006**

- **Fornasiero, A.**, Alberoni, P. P., Amorati, R., Ferraris, L., Taramasso, A. C. "Effects of propagation conditions on radar beam-ground interaction: impact on data quality", Adv. Geosci. 2: 201–208, **2005**
- **Franco, M.**; Sempere-Torres, D., Sánchez-Diezma, R. and Andrieu, H. "A methodology to identify the vertical profile of reflectivity from radar scans and to estimate the rainrate at ground at different distances", *Proc*. *ERAD 2002*, 299–304, **2002**
- **Friedrich, K.**, Hagen, M., and Einfalt, T. "A quality control concept for radar reflectivity, polarimetric parameters, and Doppler velocity", J. Atmos. Ocean. Tech., 23, pp. 865–887, **2006**
- **Fulton, R. A**., Breidenbach, J. P., Seo, D., Miller, D. and O'Bannon, T. The WSR-88D rainfall algorithm. Wea. Forecasting, 13, 377–395, **1998**
- **Gekat, F.,** Meischner, P., Friedrich, K., Hagen, M., Koistinen, J., Michelson, D. B. and Huuskonen, A. "The state of weather radar operations, networks and products", In: *Weather radar*. *Principles and advanced applications*, P. Meischner, (Ed.), 1–51, Springer-Verlag, ISBN 3-540-000328-2, Berlin – Heidelberg, Germany, **2004**
- **Germann, U.** & Joss, J., "Operational measurement of precipitation in mountainous terrain", In: *Weather radar*. *Principles and advanced applications*, P. Meischner, (Ed.), 52– 77, Springer-Verlag, ISBN 3-540-000328-2, Berlin – Heidelberg, Germany, **2004**
- **Goltz, C.,** Einfalt, T. and Galli, G. "Radar data quality control methods in VOLTAIRE", Meteorologische Zeitschrift, Vol. 15, pp. 497–504, ISSN 1610-1227, **2006**
- **Hossain, F.,** Anagnostou, E. N., Dinku, T. and Borga, M. "Hydrological model sensitivity to parameter and radar rainfall estimation uncertainty", Hydrol. Process., 18, 3277–3299, doi:10.1002/hyp.5659, **2004**
- **Jurczyk, A.**, Szturc J. and Osrodka K., "Radar rainfall compositing: comparison of different methods", Proceedings 10th European Conference on Radar in Meteorology and Hydrology (ERAD), **2018**
- **Junyent, F.** et al. "The CASA Integrated Project 1 Networked Radar System" Journal of atmospheric and oceanic technology, DOI: 10.1175/2009JTECHA1296.1, **2010**
- **Lakshmanan, V.** and Humphrey T. W. "A MapReduce Technique to Mosaic Continental-Scale Weather Radar Data in Real-time", IEEE J. Sel. Top. Appl. Earth Obs. Remote Sens., 7, 721–732, **2014**
- **Maesaka, T**. et al. "Operational rainfall estimation by x-band mp radar network in MLIT, Japan" in 35th Conference on Radar Meteorology, September **2011**
- **Maki, M.**, Maesaka, T., Kato A., Kim D. S. and Iawanami K. "Developing a composite rainfall map based on observations from an X-band polarimetric radar network and conventional C-band radar", NISCAIR-CSIR, India, vol. 41, pp. 461-470, August **2012**
- **Marzano, F. S.**, Ronzoni, M., Montopoli, M., Di Fabio, S., Picciotti, E. and Vulpiani, G. "Statistical characterization of C-band single-polarization radar retrieval space-time error in complex orography" Proc. of ERAD2012, Tolouse (France), 25-29 June **2012**
- **Marzano, F. S.**, Picciotti, E. and Vulpiani, G. "Rain field and reflectivity vertical profile reconstruction from C-band radar volumetric data", IEEE Trans. Geosci. Rem. Sens., vol. 42, n. 4, pp. 1033-1046, **2004**
- **Meischner, P.** "Weather radar. Principles and advanced applications", Springer- Verlag, ISBN 3-540-000328-2, Berlin – Heidelberg, Germany, **2004**

- **Michelson, D.** Einfalt, T.; Holleman, I.; Gjertsen, U.; Friedrich, K.; Haase, G.; Lindskog, M. & Jurczyk, A. "Weather radar data quality in Europe – quality control and characterization", Review. COST Action 717, ISBN 92-898-0018-6, Luxembourg, **2005**
- **Osrodka, K**., Szturc, J. and Jurczyk, A. "Chain of data quality algorithms for 3-D single-polarization radar reflectivity (RADVOL-QC system)", Meteorol. Appl., DOI: 10.1002/met.1323, **2012**
- **Peura, M.**, and Koistinen, J. "Using radar data quality in computing composites and nowcasting products" 33rd Conference on Radar Meteorology, Cairns, Australia, American Meteorological Society, **2007**
- **Picciotti E.**, Di Fabio, S., Barbieri, S., Montopoli, M., Zauri, R., Cipollone, A., Rossi, F. L. and Marzano F. S. "Implementation and operational use of a heterogeneous radar network in the complex orography of Abruzzo region", Proceedings 10th European Conference on Radar in Meteorology and Hydrology (ERAD), **2018**
- **Picciotti, E.** et al. "The ADRIARadNet project: ADRIAtic integrated RADar-based and web-oriented information processing system NETwork to support hydrometeorological monitoring and civil protection decision" Proc. ERAD2014, Garmisch-Partenkirchen (Germany), 1-5 September **2014**
- **Picciotti, E**. et al. "Coupling X-band dual-polarized mini-radars and hydro-meteorological forecast models: the HYDRORAD project", Nat. Hazards and Earth Syst. Sciences, vol. 13, pp. 1229-1241, **2013**
- **Rinollo, A.** et al. "Definition and impact of a quality index for radar-based reference measurements in the H-SAF precipitation product validation" Nat. Hazards Earth Syst. Sci., 13, 2695-2705 **2013**
- **Šálek, M.,** Cheze, J.-L., Handwerker, J., Delobbe, L. and Uijlenhoet, R. "Radar techniques for identifying precipitation type and estimating quantity of precipitation", COST Action 717. Luxembourg, **2004**
- **Sauvageot, H**. "Radar Meteorology". Artech House, Norwood, **1992**
- **Shepard, D.** "A two-dimensional interpolation function for irregular-spaced data", Proceedings 23rd National conference of Association for Computing Machinery (ACM), pp. 517-524, **1968**
- **Tabary, P.** "The new French operational radar rainfall product. Part I: methodology", Weather Forecast., 22, 393– 408, **2007**
- **Vulpiani, G.** and other authors "The Italian radar network within the national early-warning system for multi-risks management" Proc. of ERAD08, Helsinki, 30 June-4 July **2008**
- **Westrelin, S**., Meriaux, P., Tabary, P. and Aubert, Y. "Hydrometeorological risks in Mediterranean mountainous areas - RHYTMME Project: Risk Management based on a Radar Network" ERAD 2012 7th European Conference on Radar in Meteorology and Hydrology, Toulouse, France, **2012**
- **Zawadzki, I.** "Sense and nonsense in radar QPE", *Proceedings of ERAD 2006: 4th European Conference on Radar in Meteorology and Hydrology*, pp. 121–124, ISBN 978- 84-8181-227-5, Barcelona, Spain, September 18-22, **2006**
- **Zhang, J.**, Howard, K., Xia, W., Langston, C., Wang, S. and Qin Y. "Three-dimensional high-resolution national radar mosaic". Preprints, 11th Conf. on Aviation, Range, and Aerospace Meteorology, Hyannis, MA, Amer. Meteor. Soc., 3.5, **2004.**

ANNEX 1. CRAMS PSEUDOCODE

CRAMS.py software is a Python package that provides a variety of routines for reading, processing, analyzing, compositing and visualizing data from weather radars.
The package is organized in a number of sub-packages (modules) roughly separated by the type of functionality they provide.
The CRAMS.py software is here described by means of the Pseudocode. For clarity, at the end of the description, the modules developed are also summarized in tabular format and the processing chain scheme is recalled.

```
# Modules to reading common radar data formats in 3d volumetric raw data
# and in 2d radar products. There are a multitude of different file formats
# for data storage and exchange, although the "Eumetnet Opera" project has
# taken steps towards harmonizing the data exchange in Europe, different
# dialects still exist in addition to a large variety of legacy formats.
# Many radar data come in complex, and sometimes proprietary binary formats
# which require a lot of expertise in handling.

    # HDF5 (Hierarchical Data Format) is a set of file formats designed to
    # store and organize large amounts of data
        from m_read_3d_h5 import f_read_3d_h5
        from m_read_2d_h5 import f_read_2d_h5


    # NetCDF (Network Common Data Form) is a set of software libraries and
    # self-describing, machine-independent data formats that support the
    # creation, access, and sharing of array-oriented scientific data
        from m_read_3d_nc import f_read_3d_nc
        from m_read_2d_nc import f_read_2d_nc


    # BUFR (Binary Universal Form for the Representation of meteorological
    # data) is a binary data format. It was designed to be portable, compact,
    # and universal. Any kind of data can be represented, along with its
    # specific spatial/temporal context and any other associated metadata
        from m_read_3d_bf import f_read_3d_bf
        from m_read_2d_bf import f_read_2d_bf


    # MS (Polar File Format) is a binary data format. It is a property format
    # of manufacturer company
        from m_read_3d_ms import f_read_3d_ms
        from m_read_2d_ms import f_read_2d_ms


# Modules for convert the radar volumes/products, read from previous
# modules, into 3d or 2d array with a structure that allows a flexible and
# powerful use in the python environment. The level and detail of meta-
# information depends on the data source.
    from m_vol3d_to_mat3d import f_vol3d_to_mat3d
    from m_prod2d_to_mat2d import f_prod2d_to_mat2d
```

```
# Modules for verify the time synchronization of radar data
    from m_verify_timesync_vol3d import f_verify_timesync_vol3d
    from m_verify_timesync_prod2d import f_verify_timesync_prod2d

# Modules for remove and correct errors and artefacts in radar data.
# Before the compositing, once a scan is fully received, the data are
# processed through a specific processing chain to eliminating,
# compensating or at least to identifying the most common error sources for
# each device. Processing by means of data correction algorithms allows the
# reduction of uncertainty in the data, whereas quality analysis
# algorithms generate a map of total quality index (TQI) that can be
# attached to the data.

    # modules for clutter and radio frequency interference removal
        # velocity filter
            from m_velocity_filter import f_velocity_filter
        # texture filter
            from m_texture_filter import f_texture_filter

    # modules for data correction
        # PBB (Partial Beam Blockage) correction
            from m_pbb_correction import f_pbb_correction
        # path attenaution correction
            from m_attenuation_correction import f_attenuation_correction

    # modules for quality analysis
        # TQI (Total Quality Informaton)
            from m_tqi_3d import f_tqi_3d
            from m_tqi_2d import f_tqi_2d


# Modules to generating weather radar 2d products focussed on extreme
# events for each individual radar

    # VMI: maximum of reflectivity. This product is useful for a quick
    #          surveillance of regions of convective precipitation to locate both
    #          mature and newly developing thunderstorm.
        from m_make_sigleradar_vmi import f_make_sigleradar_vmi

    # CSD: convective storm detection. The product is aimed at distinguish
    #          stratiform and convective areas being the latter more dangerous
        from m_make_sigleradar_csd import f_make_sigleradar_csd

    # SRI, SRT: precipitation estimation. Precipitation products estimate the
    #                  ground instantaneous and accumulated rainfall over radar area
    #                  coverage. This product can issue warnings if the precipitation
    #                  in a subcatchment region exceeds a threshold value
        from m_make_sigleradar_sri import f_make_sigleradar_sri
        from m_make_sigleradar_srt import f_make_sigleradar_srt

    # VIL: vertically integrated liquid. The VIL value at a certain location
    #          is the sum of all observed radar reflectivities (converted to
```

```
    #           liquid water content) in a vertical column above this location.
    #           This product can be used as a measure for the potential strong
    #           rainfall
        from m_make_sigleradar_vil import f_make_sigleradar_vil

    # POH: hail detection. The product is aimed at hail detection which is
    #           one of the most danger phenomena
        from m_make_sigleradar_poh import f_make_sigleradar_poh

    # NOW: short time prediction of rainy filed or nowcasting. The product is
    #           aimed at short-term forecast of convective cells motion
        from m_make_sigleradar_now import f_make_sigleradar_now


# Modules to generating a radar composite
    # modules to resampling a weather radar 2d products to a common 2d grid

        # VMI: maximum of reflectivity
            from m_resampling_vmi_on_common_grid import
                                                    f_resampling_vmi_on_common_grid

        # CSD: convective storm detection
            from m_resampling_csd_on_common_grid import
                                                    f_resampling_csd_on_common_grid

        # SRI, SRT: precipitation estimation
            from m_resampling_sri_on_common_grid import
                                                    f_resampling_sri_on_common_grid
            from m_make_srt_on_common_grid import f_make_srt_on_common_grid

        # VIL: vertically integrated liquid
            from m_resampling_vil_on_common_grid import
                                                    f_resampling_vil_on_common_grid

        # POH: hail detection
            from m_resampling_poh_on_common_grid import
                                                    f_resampling_poh_on_common_grid

        # NOW: short time prediction of rainy filed or nowcasting
            from m_resampling_now_on_common_grid import
                                                    f_resampling_now_on_common_grid
```

```
# module for radar composite. Combining data from several radar locations
# on one common grid is usually referred to as composition. Creating
# composites are particularly challenging in areas where several radar
# circles overlap. In these regions of overlap, the module applies
# some criteria related to data quality in order to weight different
# radar data sources:

    # method = 1: mean. Assign the mean value of the available measurements
                  to the single point of the common grid

    # method = 2: max. Assign the maximum value of the available
                  measurements to the single point of the common grid

    # method = 3: nearest linear weighted. Assign to the common pixel of
                  the common grid a value weighted with the distance from
                  the radars, using linear weighting functions

    # method = 4: nearest exponential weighted. Assign to the common pixel
                  of the common grid a value weighted with the distance
                  from the radars, using exponential weighting functions

    # method = 5: nearest inverse distance weighted. Assign to the common
                  pixel of the common grid a value weighted by a defined
                  inversely proportional power of the distance from the
                  radar

    # method = 6: max quality. Assign to the common pixel the value
                  corresponding to the maximum final quality (tqi)

    # method = 7: minimum pia. Assign to the common pixel the value
                  corresponding to the minimum path integrated attenuation
                  (pia)

    # method = 8: weighted quality. Assign to the single point of the
                  common grid a value weighed by the final quality (tqi)
                  associated with the various radars

    # method = 9: minimum distance. Assign to the common pixel the value
                  corresponding to the minimum distance

    # method = 10: nearest quadratic weighted. Assign to the single point
                    of the common grid a value that is weighed quadratically
                    with the distance from the cell of the single radar
                    contributions

    # method = 11: weighted quality + exponential distance. Assign to the
                    common pixel of the common grid a value weighted with
                    the final quality (tqi) and a defined inversely
                    proportional power of the distance from the radar
    from m_generate_composite import f_generate_composite
```

```
# Modules for visualization weather radar 2d products focussed on extreme
# events for each individual radar and 2d composite products.

    # visualization 2d radar products

        # VMI: maximum of reflectivity
            from m_pltimg_singleradar_vmi import f_pltimg_singleradar_vmi

        # CSD: convective storm detection

            from m_pltimg_singleradar_csd import f_pltimg_singleradar_csd

        # SRI, SRT: precipitation estimation
            from m_pltimg_singleradar_sri import f_pltimg_singleradar_sri
            from m_pltimg_singleradar_srt import f_pltimg_singleradar_srt

        # VIL: vertically integrated liquid
            from m_pltimg_singleradar_vil import f_pltimg_singleradar_vil

        # POH: hail detection
            from m_pltimg_singleradar_poh import f_pltimg_singleradar_poh

        # NOW: short time prediction of rainy filed or nowcasting
            from m_pltimg_singleradar_now import f_pltimg_singleradar_now


    # visualization 2d composite products

        # VMI: maximum of reflectivity
        from m_pltimg_msc_vmi import f_pltimg_msc_vmi

        # CSD: convective storm detection
        from m_pltimg_msc_csd import f_pltimg_msc_csd

        # SRI, SRT: precipitation estimation
        from m_pltimg_msc_sri import f_pltimg_msc_sri
        from m_pltimg_msc_srt import f_pltimg_msc_srt

        # VIL: vertically integrated liquid
        from m_pltimg_msc_vil import f_pltimg_msc_vil

        # POH: hail detection
        from m_pltimg_msc_poh import f_pltimg_msc_poh

        # NOW: short time prediction of rainy filed or nowcasting
        from m_pltimg_msc_now import f_pltimg_msc_now
```

```
Start
    # for each radar in the network specify the information:
    # (‘radar name’, ‘operating frequency’, ‘3d volume or 2d product’,
    # ‘range km’, ‘file format’, ‘name file data to load’, ‘radar is on/off’)
    # An example:
        radar_list =
            [(‘Radar1’, ‘C’, ‘3d’, ‘120’, ‘hdf5’, ‘20181201_0100utc.h5’, ‘on’),
             (‘Radar2’, ‘X’,’2d’,’108’, ‘netcdf’, ‘20181201_0100utc.nc’,’off’),
              . . .,
             (‘RadarNxM’, ‘C’, ‘3d’,’60’,’bufr’, ‘20181201_0100utc.bufr’, ‘on’)]

    # reference date/time for synchronization of radar data
        ref_datetime_sync = now()

    # for each radar in the ‘radar_list’:
        # 3d volumetric raw data:
            # - read data
            # - verify the synchronization of radar data
            # - convert the radar data into a python 3d array
            # - data remove errors and artefacts
            # - data correction
            # - quality analysis
            # - generation weather radar 2d products
            # - resampling weather radar 2d products to a common 2d grid
        # 2d products data:
            # - read data
            # - verify the synchronization of radar data
            # - convert the radar product into a python 2d array
            # - quality analysis
            # - resampling weather radar 2d products to a common 2d grid
        for val_radar in radar_list:
            if ‘radar is on’ == ‘True’:
                if ‘3d volume or 2d product’ == ‘3d’:
                    # 3d volumetric raw data
                        # read data
                            if ‘file format’ == ‘hdf5’:
                                vol_read = f_read_3d_h5(‘/dir/name file to load’)
                            elif ‘file format’ == ‘netcdf’:
                                vol_read = f_read_3d_nc(‘/dir/name file to load’)
                            elif ‘file format’ == ‘bufr’:
                                vol_read = f_read_3d_bf(‘/dir/name file to load’)
                            elif ‘file format’ == ms’:
                                vol_read = f_read_3d_ms(‘/dir/name file to load’)
                        # verify the synchronization of radar data
                            flag_sync3d = f_verify_timesync_vol3d(vol_read, ref_datetime_sync)
                        if flag_sync3d == ‘True’:
                            # convert the radar data into a 3d array
                                mat3d = f_vol3d_to_mat3d(vol_read)
                                del(vol_read)
```

```
# data remove errors and artefacts
    # clutter and radio frequency interference removal with
    # velocity and texture filter
        mat3d.z = f_velocity_filter(mat3d.z, mat3d.v)
        mat3d.z = f_texture_filter(mat3d.z)
# data correction
    # Partial Beam Blockage and Path Attenuation corrections
        mat3d.z = f_pbb_correction(mat3d.z)
        mat3d.z = f_attenuation_correction(mat3d.z)
# quality analysis
    mat3d.tqi = f_tqi_3d(mat3d)

# generation weather radar 2d products
    # VMI: maximum of reflectivity
        mat2d.vmi, mat2d.tqi_vmi  =
                            f_make_sigleradar_vmi(mat3d.z, mat3d.tqi)
    # CSD: convective storm detection
        mat2d.csd, mat2d.tqi_csd =
                                f_make_sigleradar_csd(mat3d.z,mat3d.tqi,
                                                      'operating frequency')
    # SRI, SRT: precipitation estimation
        mat2d.sri, mat2d.tqi_sri =
                                        f_make_sigleradar_sri(mat2d.vmi,
                                                    mat2d.tqi_vmi,
                                                      mat2d.csd,
                                                        mat2d.tqi_csd
                                                          'operating frequency')
        mat2d.srt1h, mat2d.srt3h,
           mat2d.srt6h, mat2d.srt12h, mat2d.srt24h =
                                    f_make_sigleradar_srt(mat2d.sri, mat2d.tqi_sri)
    # VIL: vertically integrated liquid
        mat2d.vil, mat2d.tqi_vil,
                            f_make_sigleradar_vil (mat3d.z, mat3d.tqi,
                                                   'operating frequency')
    # POH: hail detection
        mat2d.poh, mat2d.tqi_poh,
                            f_make_sigleradar_vil (mat3d.z, mat3d.tqi,
                                                   'operating frequency')
    # NOW: short time prediction of rainy filed or nowcasting
        mat2d.now, mat2d.tqi_now,
                                        f_make_sigleradar_now (mat2d.vmi,
                                                               mat2d.tqi_vmi)
# resampling weather radar 2d products to a common 2d grid
    # VMI: maximum of reflectivity
        mat2d.msc_vmi, mat2d.msc_tqi_vmi =
                            f_resampling_vmi_on_common_grid(mat2d.vmi,
                                                            mat2d.tqi_vmi,
                                                              'range km')
```

```
                # CSD: convective storm detection
                    mat2d.msc_csd, mat2d.msc_tqi_csd =
                                    f_resampling_csd_on_common_grid(mat2d.csd,
                                                                    mat2d.tqi_csd,
                                                                      'range km')
                # SRI, SRT: precipitation estimation
                    mat2d.msc_sri, mat2d.msc_tqi_sri =
                                    f_resampling_sri_on_common_grid(mat2d.sri,
                                                                    mat2d.tqi_sri,
                                                                      'range km')
                # VIL: vertically integrated liquid
                    mat2d.msc_vil, mat2d.msc_tqi_vil =
                                    f_resampling_vil_on_common_grid(mat2d.vil,
                                                                    mat2d.tqi_vil,
                                                                      'range km')
                # POH: hail detection
                    mat2d.msc_poh, mat2d.msc_tqi_poh =
                                    f_resampling_poh_on_common_grid(mat2d.poh,
                                                                    mat2d.tqi_poh,
                                                                      'range km')
                # NOW: short time prediction of rainy filed or nowcasting
                    mat2d.msc_now, mat2d.msc_tqi_now =
                                    f_resampling_now_on_common_grid(mat2d.now,
                                                                    mat2d.tqi_now,
                                                                      'range km')
                    val_radar.append(mat3d)
                    val_radar.append(mat2d)
            elif flag_sync3d == 'False':
                # the date of radar volume is out of time
                    val_radar[6] = 'off'
                    mat3d = nan
                    mat2d = nan
                    val_radar.append(mat3d)
                    val_radar.append(mat2d)
            del(mat3d)
            del(mat2d)
    elif '3d volume or 2d product' == '2d':
        # 2d products data
            # read data
                if 'file format' == 'hdf5':
                    prod_read = f_read_2d_h5('/dir/name file to load')
                elif 'file format' == 'netcdf':
                    prod_read = f_read_2d_nc('/dir/name file to load')
                elif 'file format' == 'bufr':
                    prod_read = f_read_2d_bf('/dir/name file to load')
                elif 'file format' == ms':
                    prod_read = f_read_2d_ms('/dir/name file to load')
            # verify the synchronization of radar data
                flag_sync2d =
                            f_verify_timesync_vol2d(prod_read,ref_datetime_sync)
            if flag_sync2d == 'True':
                mat3d = nan
                # convert the radar products into a 2d array
```

```
                mat2d.vmi, mat2d.csd, mat2d.sri, mat2d.srt1h,
                    mat2d.srt3h, mat2d.srt6h, mat2d.srt12h
                        mat2d.srt24h, mat2d.vil, mat2d.poh,
                                                mat2d.now =
                                                    f_prod2d_to_mat2d(prod_read)
                del(prod_read)
            # quality analysis
                mat2d.tqi_vmi, mat2d.tqi_csd, mat2d.tqi_sri,
                    mat2d.tqi_vil, mat2d.tqi_poh,
                                        mat2d.tqi_now = f_make_TQI_2d(mat2d)
            # resampling weather radar 2d products to a common 2d grid
                # VMI: maximum of reflectivity
                    mat2d.msc_vmi, mat2d.msc_tqi_vmi =
                                f_resampling_vmi_on_common_grid(mat2d.vmi,
                                                                ,mat2d.tqi_vmi,
                                                                  'range km')
                # CSD: convective storm detection
                    mat2d.msc_csd, mat2d.msc_tqi_csd =
                                    f_resampling_csd_on_common_grid(mat2d.csd,
                                                                mat2d.tqi_csd,
                                                                  'range km')
                # SRI, SRT: precipitation estimation
                    mat2d.msc_sri, mat2d.msc_tqi_sri =
                                    f_resampling_sri_on_common_grid(mat2d.sri,
                                                                mat2d.tqi_sri,
                                                                  'range km')
                # VIL: vertically integrated liquid
                    mat2d.msc_vil, mat2d.msc_tqi_vil =
                                    f_resampling_vil_on_common_grid(mat2d.vil,
                                                                mat2d.tqi_vil,
                                                                  'range km')
                # POH: hail detection
                    mat2d.msc_poh, mat2d.msc_tqi_poh =
                                    f_resampling_poh_on_common_grid(mat2d.poh,
                                                                mat2d.tqi_poh,
                                                                  'range km')
                # NOW: short time prediction of rainy filed or nowcasting
                    mat2d.msc_now, mat2d.msc_tqi_now =
                                    f_resampling_now_on_common_grid(mat2d.now,
                                                                mat2d.tqi_now)
                    val_radar.append(mat3d)
                    val_radar.append(mat2d)

            elif flag_sync2d == 'False':
                # the date of radar product is out of time
                    val_radar[6] = 'off'
                    mat3d = nan
                    mat2d = nan
                    val_radar.append(mat3d)
                    val_radar.append(mat2d)
            del(mat3d)
            del(mat2d)
    elif 'radar is on' == 'False':
```

```
            mat3d = nan
            mat2d = nan
            val_radar.append(mat3d)
            val_radar.append(mat2d)
            del(mat3d)
            del(mat2d)

    # generation radar composite, combining data from several radar locations
    # on one common grid
        msc2d.vmi, msc2d.csd, msc2d.sri, msc2d.vil,
                                                msc2d.poh, msc2d.now =
                                                    f_make_composite(radar_list, method)
        # SRT1h, SRT3h, SRT6h, SRT12h, SRT24h
            msc2d.srt1h, msc2d.srt3h, msc2d.srt6h,
                                    msc2d.srt12h, msc2d.srt24h =
                                                f_make_srt_on_common_grid(msc2d.sri)

    # visualization weather radar 2d products focused on extreme events for
    # each individual radar and 2d composite products.
        # 2d radar products
            for val_radar in radar_list:
                if 'radar is on' == 'True':
                    f_pltimg_singleradar_vmi(val_radar)
                    f_pltimg_singleradar_csd(val_radar)
                    f_pltimg_singleradar_sri(val_radar)
                    f_pltimg_singleradar_srt(val_radar)
                    f_pltimg_singleradar_vil(val_radar)
                    f_pltimg_singleradar_poh(val_radar)
                    f_pltimg_singleradar_now(val_radar)

        # 2d composite products
            f_pltimg_msc_vmi(msc2d)
            f_pltimg_msc_csd(msc2d)
            f_pltimg_msc_sri(msc2d)
            f_pltimg_msc_srt(msc2d)
            f_pltimg_msc_vil(msc2d)
            f_pltimg_msc_poh(msc2d)
            f_pltimg_msc_now(msc2d)
End
```

Modules	Purpose	General Description
• m_read_3d_h5 • m_read_2d_h5	read radar data	Hierarchical Data Format (HDF5)
• m_read_3d_nc • m_read_2d_nc		Network Common Data Form (NetCDF)
• m_read_3d_bf • m_read_2d_bf		Binary Universal Form for the Representation of meteorological data (BUFR)
• m_read_3d_ms • m_read_2d_ms		Polar File Format (MS)
• m_vol3d_to_mat3d • m_prod2d_to_mat2d	convert radar data	convert radar data into a python 2d/3d array
• m_verify_timesync_vol3d • m_verify_timesync_prod2d	verify synchronization	verify the timing of radar data
• m_velocity_filter • m_texture_filter	remove and correct errors and artefacts in radar data	clutter and radio frequency interference
• m_pbb_correction • m_attenuation_correction		partial beam blockage and path attenuation correction
• m_tqi_3d • m_tqi_2d		quality analysis
• m_make_sigleradar_vmi	generate weather radar 2d products for individual radar	maximum of reflectivity
• m_make_sigleradar_csd		convective storm detection
• m_make_sigleradar_sri • m_make_sigleradar_srt		precipitation estimation
• m_make_sigleradar_vil		vertically integrated liquid
• m_make_sigleradar_poh		hail detection
• m_make_sigleradar_now		short time prediction rainy
• m_resampling_vmi_on_common_grid	resampling weather radar 2d products to common 2d grid	maximum of reflectivity
• m_resampling_csd_on_common_grid		convective storm detection
• m_resampling_sri_on_common_grid • m_make_srt_on_common_grid		precipitation estimation
• m_resampling_vil_on_common_grid		vertically integrated liquid
• m_resampling_poh_on_common_grid		hail detection
• m_resampling_now_on_common_grid		short time prediction rainy
• m_generate_composite	Generate a radar composite	combine data from several radar locations on the common 2d grid
• m_pltimg_singleradar_vmi	visualization weather radar 2d products for individual radar	maximum of reflectivity
• m_pltimg_singleradar_csd		convective storm detection
• m_pltimg_singleradar_sri • m_pltimg_singleradar_srt		precipitation estimation

	• m_pltimg_singleradar_vil		vertically integrated liquid
	• m_pltimg_singleradar_poh		hail detection
	• m_pltimg_singleradar_now		short time prediction rainy
	• m_pltimg_msc_vmi	visualization weather radar 2d composite products	maximum of reflectivity
	• m_pltimg_msc_csd		convective storm detection
	• m_pltimg_msc_sri • m_pltimg_msc_srt		precipitation estimation
	• m_pltimg_msc_vil		vertically integrated liquid
	• m_pltimg_msc_poh		hail detection
	• m_pltimg_msc_now		short time prediction rainy